Geomorphology 417 (2022) 108451

Contents lists available at ScienceDirect

Geomorphology

journal homepage: www.journals.elsevier.com/geomorphology

Poljes in the Sivas gypsum karst, Turkey

Ergin Gökkaya [a,*], Francisco Gutiérrez [b]

[a] Department of Geography, Ankara University, Turkey, 06100 Ankara, Turkey
[b] Department of Earth Sciences, University of Zaragoza, 50009 Zaragoza, Spain

ARTICLE INFO

Keywords:
Gypsum polje
Base-level polje
Corrosion planation
Solutional undercutting
Groundwater flooding
Floodwater cave

ABSTRACT

Karst poljes, despite their large dimensions and significant applied interest, have received limited attention in the geomorphological literature, and references to gypsum poljes are incidental. This work analyses the morpho-structural setting, characteristics, origin and controlling factors of thirteen poljes mapped in the gypsum karst of Sivas, Turkey. The poljes occur along a 38 km long belt associated with the allogenic Kızılırmak and Acısu rivers, which constitute the regional base level of the karst system. The path of these drainages is controlled by the trailing morpho-structural trough of the antiformal ridge associated with the front of the active Sivas Thrust. The floor of most of the poljes is connected with the floodplain of the main rivers, but largely lies at lower elevation, functioning as semi-closed basins that can be flooded by water table rise and the incorporation of floodwaters from the adjacent fluvial systems. The depressions, with their floors situated within the epiphreatic zone, are classified as base-level poljes. Three types of base-level poljes are differentiated based on cartographic relationships and attending to their evolutionary path: poljes associated with relict valleys; poljes developed in abandoned valley sections, poljes related to the coalescence of bedrock collapse sinkholes. The poljes expand by lateral solution planation, involving the retreat of the marginal slopes and their replacement by a solution plain (polje floor) controlled by the water table. The retreat of the slopes is mainly achieved by solutional undercutting during floods, mass movements, and the rapid removal of the gypsiferous landslide deposits. These processes are expected to operate in gypsum bedrock at much higher rates than in carbonate rocks. Dissolution acting at the foot of the scarped gypsum slopes during floods locally produce floodwater footcaves with the typical water injection features (e.g., spongework, solution pockets, tapering dead-end passages). These caves locally produce bedrock collapse sinkholes that can be incorporated into the polje depressions generating characteristic embayments. The main factors that seem to favor the development of poljes in Sivas include: (1) a morpho-structural trough with relatively low uplift rate that confined the path of the main drainages; (2) abundant aggressive water supplied by allogenic rivers; (3) a fluviokarst landscape including fluvial landforms that can transform into poljes; and (4) presence of clusters of bedrock collapse sinkholes that experience rapid expansion.

1. Introduction

Poljes are large depressions in karst terrain characterized by flat floors underlain by unconsolidated deposits, underground drainage, and commonly an elongated shape controlled by the structural geological grain (Sweeting, 1972; Gams, 1978; Ford and Williams, 2007; De Waele and Gutiérrez, 2022 and references therein). Poljes are mostly topographically enclosed basins that may receive water inflow from springs, autogenic and allogenic runoff, and direct precipitation, whereas the water mostly leaves the depressions via ponors (i.e. swallow holes) and diffuse infiltration (Bonacci, 1987). Flooding often occurs in the polje floors due to the water table rise or when the water entering the polje exceeds the drainage capacity of the ponors and infiltration zones (e.g., Sweeting, 1972; López-Chicano et al., 2002; Blatnik et al., 2017; Bayrakdar et al., 2020). The former (groundwater flooding) occurs when the floor of the poljes is situated within the epiphreatic zone.

In a recent work, De Waele and Gutiérrez (2022) proposed a genetic classification of poljes inspired by previous classifications (Sweeting, 1972; Gams, 1978, 1994; Ford and Williams, 2007) and taking into consideration the key role played by active faulting in the formation of numerous poljes. This classification differentiates two main genetic groups: (1) Neotectonic poljes, which are fault-bounded tectonic basins with a thick sedimentary fill, but with underground drainage through karst formations (e.g., Mijatović, 1984; Gracia et al., 2003; Aiello et al.,

* Corresponding author at: Ankara University, Faculty of Languages History and Geography, Geography Department No:45-45/A 06100 – Sıhhiye, Ankara, Turkey.
E-mail addresses: egokkaya@ankara.edu.tr (E. Gökkaya), fgutier@unizar.es (F. Gutiérrez).

https://doi.org/10.1016/j.geomorph.2022.108451
Received 24 May 2022; Received in revised form 2 September 2022; Accepted 12 September 2022
Available online 16 September 2022

2007; Sanz de Galdeano, 2013; Doğan et al., 2017, 2019 and references therein); (2) Erosional poljes that mainly result from differential erosion, mainly solutional denudation acting on karst rocks. Erosional poljes, depending on their geological and hydrological setting can be classified into base-level poljes, border poljes and overflow poljes, which are not exclusive categories that may show some overlap. Base-level poljes initiate when the ground surface reaches the epiphreatic zone by solutional lowering, and subsequently expand by lateral solution planation through the retreat of the slopes at the margins, generating flat floors controlled by the water table. Border poljes result for differential solutional lowering acting on karst rocks in contact with impermeable rocks (i.e. contact karst). These poljes are generally asymmetric and receive substantial allogenic runoff from the margin underlain by non-karst rocks (e.g., Gracia et al., 2002). Overflow poljes are largely underlain by impermeable bedrock, but water inflow and outflow are generally achieved via springs and ponors located on karst rocks at the margins (e.g., Gams, 1978; Stepišnik et al., 2012).

Flat-floored poljes, which interrupt the often rugged and unproductive rock outcrops of karst areas, have significant societal and economic importance. They host extensive agricultural lands, concentrate population and infrastructure, and may provide direct access to water, in some cases managed by major engineering projects (Milanovic, 2002, 2018; Bonacci, 2013). However, in spite of their large dimensions (up to hundreds of square kilometers) and importance for human development, they are one of the less understood surface landforms in karst (De Waele and Gutiérrez, 2022). Moreover, the vast majority of the scarce geomorphological investigations on poljes are focused on carbonate rocks and references to gypsum poljes are incidental (Gutiérrez and Cooper, 2013). Probably, this is the reason why poljes are often defined as depressions endemic to carbonate karst (e.g., Field, 2002; Bonacci, 2004, 2013). Sauro (1996) referred to several polje-like depressions in gypsum, but without providing information on their origin (e.g., sinkhole coalescence, dissolution-induced subsidence, solution planation). In two diapirs of Triassic evaporites of the Betics, southern Spain, Calaforra and Pulido-Bosch (1999) designated some large flat-floored depressions as poljes. Most probably these are subsidence basins related to evaporite dissolution beneath the caprock of the diapir. In the Iberian Chain, Spain, Garay (2001) refers to the 1.1 km long Prado de las Lagunas polje developed on Triassic evaporites. This depression, located 1 km south of Segorbe village, is sporadically flooded and drained through ponors (Gutiérrez et al., 2008a). Nicod (2006) described some large depressions that host lakes (Bonne Cougne Pond in southern France, several depressions in the Middle Atlas of Morocco) as poljes in his review on lakes associated with gypsum bedrock in Alpine and Mediterranean countries. Nonetheless, as Nicod (2006) explains, these are subsidence basins related to interstratal dissolution of Triassic evaporites. De Waele et al. (2017) reports on large structurally-controlled polje-like depressions in outcrops of Messinian gypsum of southern Sicily. These basins, either open or closed, are characterized by flat floors with alluvial and lacustrine deposits and steep slopes. The extensive gypsum outcrops of Sivas in Turkey display exceptional and rare examples of karst and fluviokarst landforms, including an outstanding polygonal karst landscape of densely packed solution sinkholes (Waltham, 2002; Doğan and Yeşilyurt, 2019; Poyraz et al., 2021), abundant bedrock collapse sinkholes of extraordinary dimensions (Gökkaya et al., 2021), long gypsum canyons (Alagöz, 1967; Doğan and Yeşilyurt, 2004, 2019; Gökkaya et al., 2021), and poljes. Some authors mentioned the presence of poljes in the Sivas gypsum karst, but no specific studies have been carried out so far. Alagöz (1967) interpreted the Tödürge depression as an uvala (compound sinkhole). Waltham (2002) suggested that some of the poljes may previously have been occupied by meander loops of rivers. Doğan and Özel (2005) proposed that poljes in the central sector of the Sivas gypsum karst are controlled by tectonic structures and result from solutional deepening and lateral planation. Doğan and Yeşilyurt (2019) suggested that the poljes are derived from an evolutionary path that involves the transformation of paleovalleys into blind valleys and then into poljes by solutional lowering and widening processes associated with the water table. The main objectives of this work, largely based on detailed geomorphological mapping and field surveys, include: (1) understanding the geological and neotectonic context in which the poljes have been developed; (2) characterizing the morphology, morphometry and hydrology of the poljes, as well as the associated caves; (3) analyzing their spatial distribution and genetic relationship with other landforms; (4) identifying the main processes involved in their formation and the resulting diagnostic landforms; and (5) assessing the main controlling factors that have allowed the development of these exceptional poljes. To our knowledge, this is the first work specifically devoted to poljes in gypsum, contributing to partially fill a significant knowledge gap in the karst literature.

2. The study area

2.1. Geological setting

The Sivas Basin, with a Late Cretaceous to Miocene fill, is a tectonically inverted sedimentary basin located in the central-eastern sector of the Anatolian microplate (Fig. 1). This microplate results from the accretion in Late Cretaceous-Paleocene times of several microcontinents along the southern margin of the Eurasian plate. The accretion of terranes was related to the closure of the northern Neotethys ocean through north-directed subductions, accompanied by south-directed obduction of ophiolites. Three continental blocks are differentiated from N to S (Fig. 1): (1) the Pontides; (2) the Kırşehir block, made up of metamorphic rocks; and (3) the Taurides, consisting of non-metamorphosed Phanerozoic sedimentary rocks. The Izmir-Ankara-Erzincan suture zone with its associated ophiolites, and the inferred (non-exposed) Inner-Tauride suture zone define the Pontides-Kırşehir and Kırşehir-Taurides boundaries, respectively (Poisson et al., 1996; Legeay et al., 2019b) (Figs. 1, 2B). Further south, the Bitlis-Zagros suture marks the boundary between the Anatolian microplate and the Arabian plate (Fig. 1). This suture results from the closure of the southern Neotethys by north-directed subduction with associated obduction in the Late Cretaceous, followed by continent-to-continent collision in the Cenozoic (McQuarrie and Hinsbergen, 2013; Darin et al., 2018). The northward-propagating shortening related to this collision produced fold-and-thrust belts in the Anatolian microplate, and controlled the development of the Sivas Basin during its synorogenic Cenozoic evolution.

The E-W oriented Sivas Basin is located astride the accreted Kırşehir and Taurides basement blocks, overlying the Inner-Tauride suture at their boundary (Figs. 1, 2B). The structure of the basin is largely controlled by a thick late Eocene salt formation (Tuzhisar Fm.), which has experienced significant synorogenic diapiric activity, remobilization (Kergaravat et al., 2016, 2017) and recycling (Pichat, 2017; Pichat et al., 2018). Two main overlapping E-W-trending structural domains are differentiated in this tectonically inverted basin, largely decoupled by the late Eocene salt detachment (Legeay et al., 2019a, 2019b) (Fig. 2B): (1) A southern and lower Fold-and-Thrust Belt (FTB), consisting of north-verging thrust sheets involving the pre-salt Taurides basement (sedimentary rocks and ophiolites) and Late Cretaceous to Eocene formations; and (2) A northern and upper salt-controlled domain, known as the Salt-and-Thrust Belt (STB), which involves the late Eocene salt and the younger Oligo-Miocene formations. This structural unit covers the northern sector of the FTB, which is roofed by the late Eocene salt. The Salt-and-Thrust Belt is in turn divided into two structural zones; the central Wall-and-Basin Structure (WABS), and the Northern Evaporitic Domain (NED), which is the area in which the investigated gypsum poljes occur. The Wall-and-Basin Structure displays (Kergaravat et al., 2016, 2017) (Fig. 2): (1) a primary generation of late Eocene-Oligocene minibasins and intervening salt walls; (2) an overlying salt canopy of remobilized salt that functions as a supplementary detachment level; and (3) a secondary generation of Oligo-Miocene minibasins developed

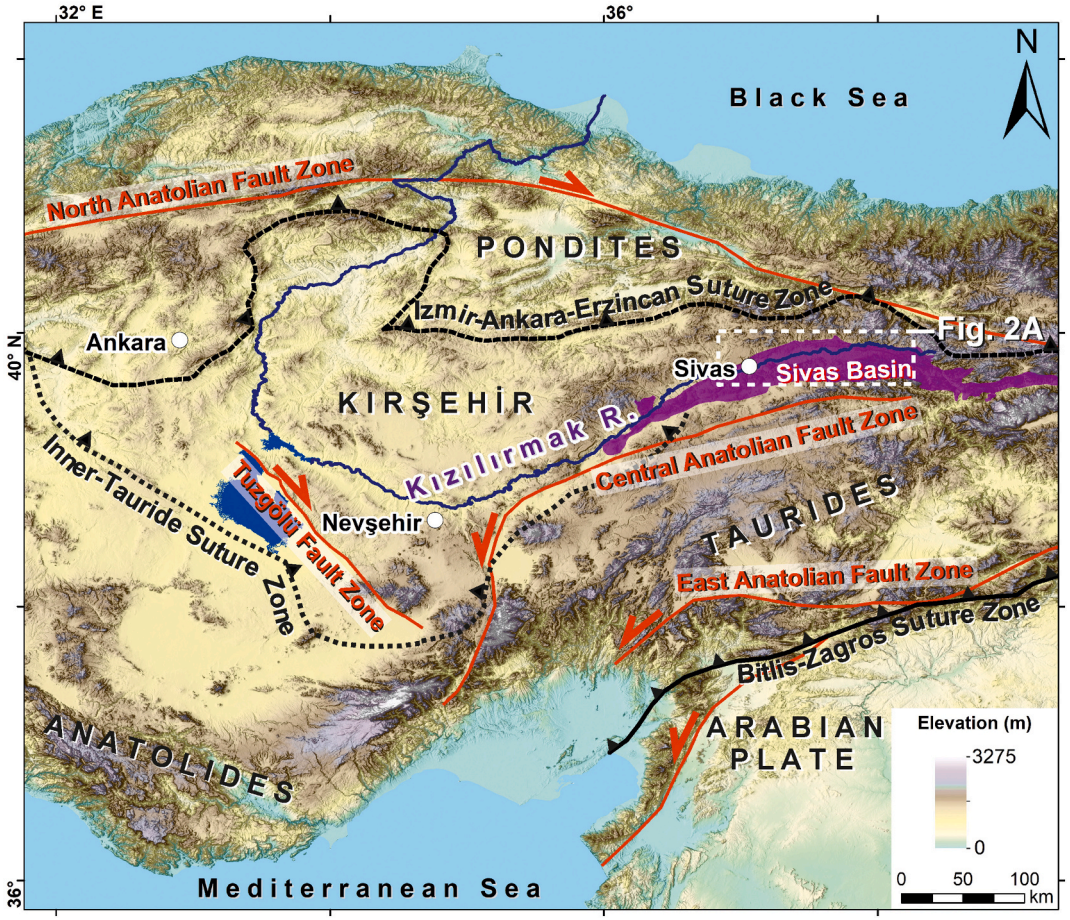

Fig. 1. Geotectonic setting of the Sivas Basin, located astride two accreted terranes within the Anatolian microplate (Kırşehir and Taurides) bounded by the Inner-Tauride suture zone.

onto the salt canopy. Shortening in the WABS domain has been accommodated by the squeezing and welding of the salt walls, the rotation and thrusting of the minibasins, and general northward and southward thrusting along the late Eocene salt, acting as a passive roof decóllement. The Northern Evaporitic Domain, bounded to the north by the N-directed Sivas Thrust (Poisson et al., 1996) and as much as 17 km wide and 100 km long, consists of an extensive outcrop of gypsum-dominated evaporites of debated age, unconformably overlain by local outliers of early Miocene marine limestones. The Kızılırmak Basin, in front of the arcuate Sivas Thrust, is the present-day foreland basin, with a wedge of Pliocene (exposed) and older (concealed) sediments onlapping the Kırşehir block to the north (Fig. 2).

The tectono-stratigraphic evolution of the central (WABS) and southern (FTB) sectors of the Sivas Basin has been reconstructed on the basis of stratigraphic and structural relationships observed in outcrops and seismic reflection profiles (Legeay et al., 2019a, 2019b). Here, we differentiate the following stages:

(I) Pre-orogenic stage (Late Cretaceous-Paleocene). The development of the basin started in the Late Cretaceous after the obduction of ophiolites associated with north-directed subductions along the Izmir-Ankara-Erzincan suture and the inferred Inner-Tauride suture zones. Shallow-platform carbonates were deposited on the ophiolites along the southern margin of the basin (Tecer Fm.), grading into turbidites and volcanoclastics in the deeper parts of the basin (Kaleköy, Konakyazı, Cercapindere Fms.).

(II) Onset of the orogenic period (Eocene). This stage was dominated by the accumulation of thick turbiditic successions (Bahçecik, Kozluca, Yapalı, Bozbel Fms.). The deposition of turbidites with olistostromes and mass flows derived from the basin margins (Bahçecik Fm.) is attributed to the start of the compression and the development of the FTB. The shortening was driven by the closure of the southern Neotethys and the convergence between the Arabian and Anatolian plates to the south.

(III) Evaporitic sedimentation (late Eocene). The north-propagating shortening caused the isolation of the foreland basin, leading to the deposition of a thick and laterally extensive salt formation (Tuzhisar Fm.; Önal et al., 1999; Gündoğan et al., 2005; Poisson et al., 2011; Pichat, 2017). The original thickness of this salt-rich unit is highly uncertain due to significant remobilization by diapiric activity, but most probably reached >1 km in thickness (Kergaravat et al., 2016, 2017).

(IV) Primary minibasins (late Eocene-middle Oligocene). Development of halokinetic minibasins with terrestrial deposits (Selimiye Fm.) by subsidence into the underlying salt, and the concomitant growth of salt walls, which fed an extrusive canopy of allochthonous salt over the basins.

(V) Secondary minibasins (middle Oligocene-late Miocene). Synorogenic growth of secondary minibasins over the salt canopy by downbuilding related to the spelling of allochthonous salt from beneath. The infill of the secondary minibasins includes the fluvio-lacustrine Karayün Fm., the marine Karacaören Fm. (late Oligocene-early Miocene) related to regional transgression, and the continental Benlikaya Fm. (Miocene) (Ribes et al., 2015, 2017).

The exposed continental sediments in the Kızılırmak foreland basin,

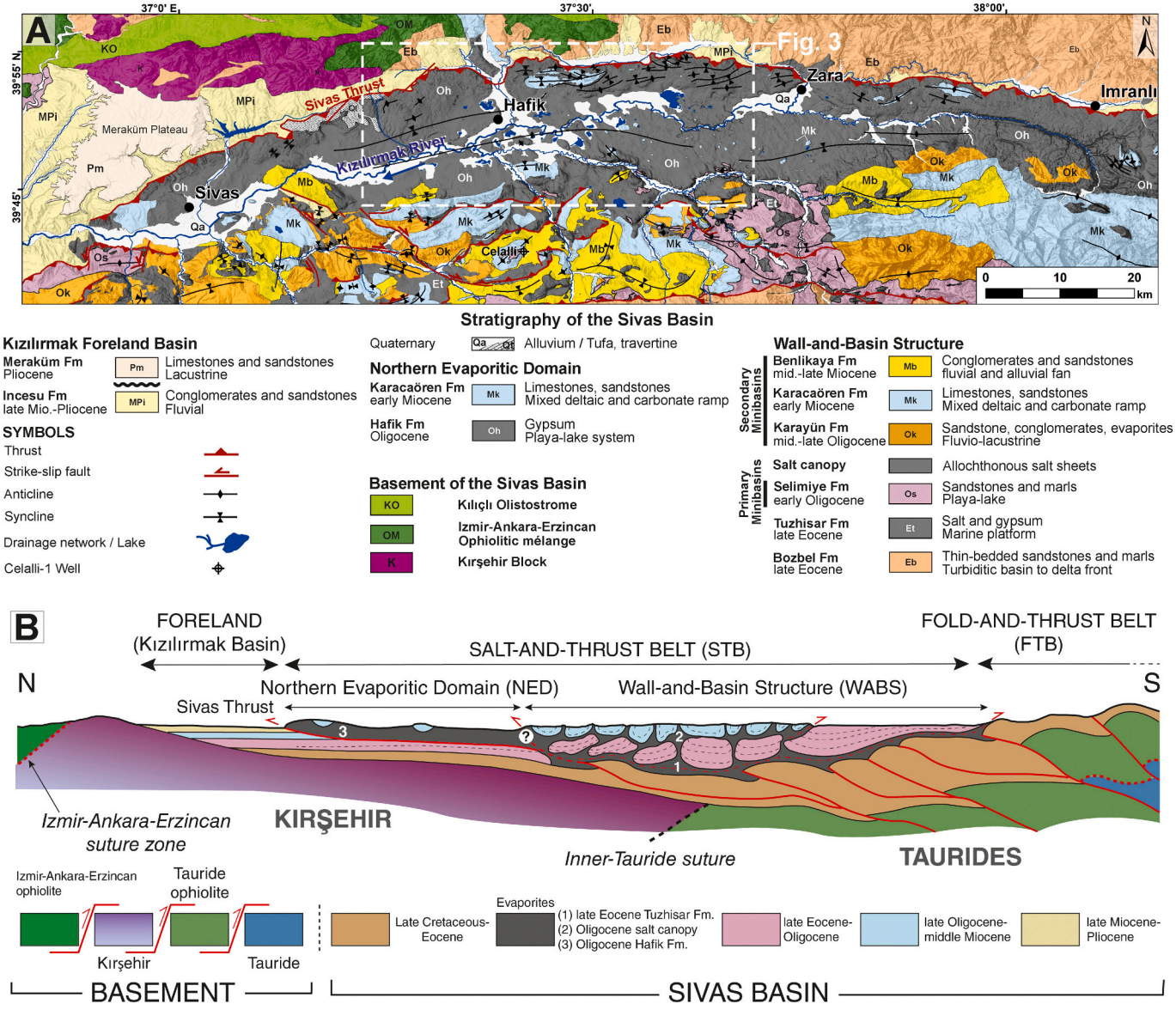

Fig. 2. Geological setting of the Sivas Basin and the study area. A: Geological map of the northern sector of the Sivas Basin covering from S to N the Wall-and-Basin Structure, the Northern Evaporitic Domain, and the Kızılırmak Foreland basin. The southern sector of the basin (Fold-and-Thrust Belt) is not shown in this map. B: Generalized cross-section of the tectonically inverted Sivas Basin showing the different structural zones and the lithological groups of the basement and basin fill. Both figures adapted from Legeay et al. (2019a, 2019b).

north of the Sivas Thrust and affected by this structure, comprise the alluvial-dominated facies of the Incesu Fm. (late Miocene-Pliocene), unconformably overlain by carbonate lacustrine deposits of the Meraküm Fm. The latter, ascribed to the Pliocene (Poisson et al., 1996), forms the caprock of the extensive NW-tilted Meraküm Plateau N of Sivas city (Fig. 2A).

The available data on the Northern Evaporitic Domain is more limited (e.g., poor quality seismic imaging; Legeay et al., 2019b) and its paleogeographic evolution is a matter of debate. Here, the exposed evaporites hundreds of meters thick mainly consist of laterally continuous gypsum beds and intercalated reddish argillaceous layers. These folded gypsum-dominated evaporites are locally overlain by remnants of early Miocene limestones of the Karacaören Fm., which also occurs in the secondary minibasins in the WABS domain. Two main interpretations have been proposed for the evaporites in this northern domain: (1) The N-directed emplacement of a large extrusive canopy of remobilized late Eocene salt before the early Miocene transgression, recorded by the overlying marine limestones of the Karacaören Fm. (Kergaravat et al., 2016, 2017). According to Kergaravat et al. (2016), this salt sheet would be rooted in the allochthonous salt separating the two generations of minibasins in the WABS domain. (2) Deposition of an Oligocene Ca-sulphate formation several hundred meters thick in an extensive evaporitic system. This unit, designated by numerous authors as the Hafik Fm., is ascribed to the Oligocene by Poisson et al. (1996, 2016), based on cartographic relationships and vertebrate fauna found in the uppermost beds (Sümengen et al., 1990). Probably, this evaporitic unit was deposited by the recycling of older evaporites in a playa-lake system associated with a former foreland basin (Pichat, 2017), and was subsequently incorporated into the orogenic wedge by the northward propagation of the deformation and the development of the Sivas Thrust. The concept of evaporite recycling in the Sivas Basin has been substantiated by Pichat et al. (2018), who demonstrated with Sr isotopic data that the units of lacustrine gypsum deposited in the secondary minibasins were derived from the dissolution of the marine late Eocene evaporites of the Tuzhisar Fm. These contrasting interpretations have important implications for understanding the gypsum karst developed in

the Northern Evaporitic Domain of the Sivas Basin. Essentially, the first alternative (remobilized unit) proposes that the evaporites are extrusive sheets of late Eocene salt, whereas the second (depositional unit) sustains that they are a different Oligocene formation. In both cases, the nature of the sediments underlying the evaporites remains uncertain. The salt canopy interpretation implicitly suggests that the Northern Evaporitic Domain should be an adequate terrain for the development of salt karst. The second interpretation (autochthonous Oligocene Ca-sulphate-dominated unit) is our preferred alternative supported by the following lines of evidence: (1) biostratigraphic data support that the evaporites are an Oligocene depositional unit younger that the Tuzhisar Fm. (Sümengen et al., 1990; Poisson et al., 2016); (2) the evaporites do not show the lithological characteristics and internal structure expected for salt sheets, which typically display intricate folding and large amounts of unstratified dissolution residues (Jackson and Hudec, 2017; Pichat et al., 2018); (3) the available hydrochemical data strongly support that the evaporites are dominated by Ca-sulphates (Kaçaroğlu et al., 2001; Günay, 2002; Gökkaya et al., 2021), in contrast with the WABS domain, where Na- and Cl-rich springs are common (Pichat et al., 2018); and (4) the area lacks geomorphic features characteristic of salt karst terrains (e.g., Frumkin, 2013; Warren, 2016; De Waele and Gutiérrez, 2022).

2.2. Morphostructural setting

The Northern Evaporitic Domain (NED), dominated by gypsum outcrops of the Oligocene Hafik Fm. (Poisson et al., 2016), is located in the hanging wall of the Sivas Thrust, between the salt-wall and mini-basin domain (WABS) to the S, and the Kızılırmak Basin, to the N (Figs. 2B, 3). The NED and the WABS are probably bounded by an N-verging thrust (Legeay et al., 2019a, 2019b) and display markedly different morphostructural features. The NED is dominated by a stepped plateau-like topography, whereas the WABS shows a rugged landscape largely attributable to differential erosion in the minibasins and the evaporites of the Late Eocene Tuzhisar Fm.. The Kızılırmak Basin is the current foreland basin of the orogenic wedge developed by the inversion of the Sivas Basin due to the Cenozoic collision between the Arabian plate and the Anatolian microplate. The youngest sediments of the dissected Mio-Pliocene fill of this basin are the lacustrine limestones of the Meraküm Fm., ascribed to the Pliocene (Poisson et al., 1996) (Fig. 2A). West of Sivas city, this unit forms the caprock of a structural platform (1650 m a.s.l.) tilted to the NNW, away for the Sivas Thrust, and perched around 400 m above the deeply entrenched Kızılırmak River (120 m a.s.l.). Gökkaya et al. (2021) estimated a long-term incision rate for this drainage of 0.11 mm yr^{-1}, assuming that the onset of fluvial dissection occurred at the base of the late Pliocene (3.6 Ma). This long-term downcutting can be ascribed to regional uplift within a compressional setting.

The boundary between the Kızılırmak Basin and the Northern Evaporitic Domain is defined by the active N-verging Sivas Thrust (Fig. 3). This 110-km-long and ENE-WSW-oriented thrust displays an arcuate trace with N-facing convexity, suggesting greater propagation of the deformation in the central sector where the orogenic wedge has a lower taper angle (Legeay et al., 2019b), attributable to a lower friction detachment (i.e., thicker evaporites?). Evidence of recent activity along the Sivas Thrust include: (1) evaporites of the Hafik Fm. overriding the Mio-Pliocene Incesu Fm. (Temiz, 1996; Poisson et al., 1996) (Fig. 2); (2) deformation of the Pliocene Meraküm Fm. (Poisson et al., 1996, 2016); (3) northward tilting of Quaternary tufa deposits associated with the Sivas Thrust NE of Sivas city (Fig. 2A); (4) geomorphic anomalies such as

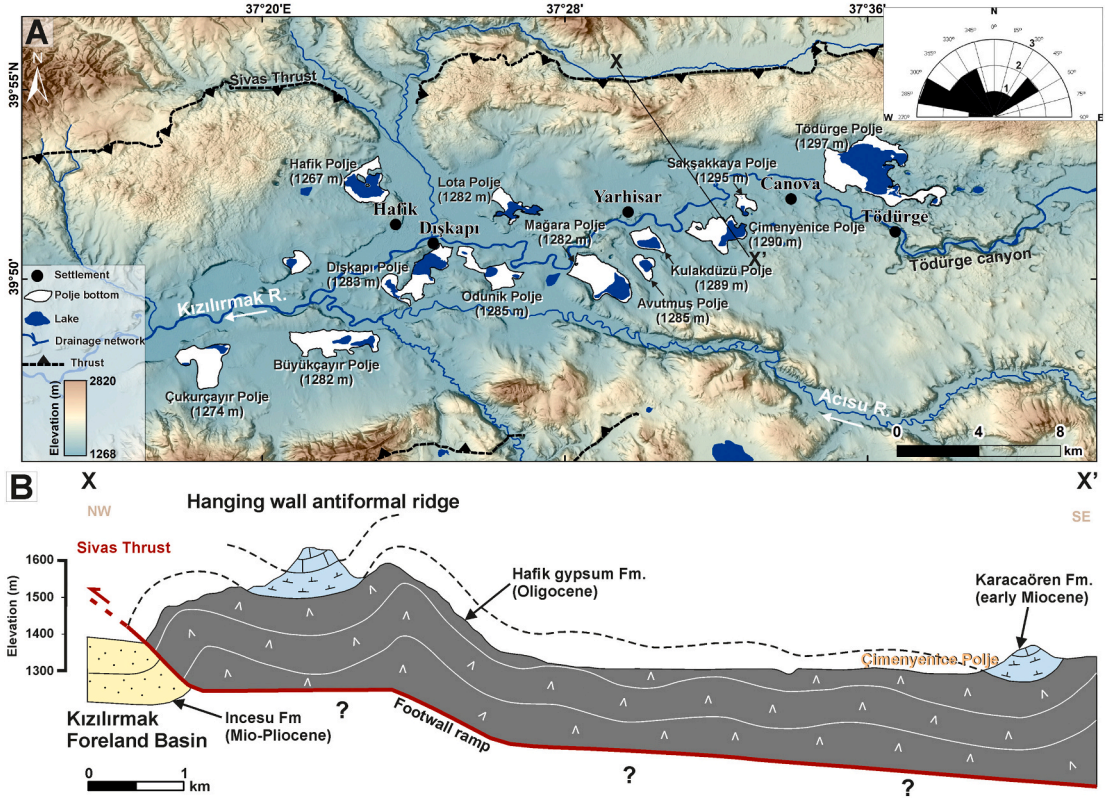

Fig. 3. Geomorphic and structural setting of the gypsum poljes. A: Shaded relief model showing the general distribution of the poljes associated with the Kızılırmak River, south of the hanging wall antiformal ridge of the Sivas Thrust. Inset rose diagram shows the frequency of the orientation of the major axis of poljes. B: Cross-section illustrating the overall structure of the Northern Evaporitic Domain, with an antiformal ridge controlled by a footwall ramp and a low-lying area at the trailing zone drained longitudinally by the Kızılırmak River. Altitudinal position of the early Miocene Karacaören Fm. records the differential uplift across the thrust sheet. (For interpretation of the references to colour in this figure legend, the reader is referred to the web version of this article.)

drainage disturbances attributable to ongoing deformation (e.g., Gökkaya et al., 2021). The Sivas Thrust locally controls longitudinal drainages in the footwall flowing along asymmetric valleys with a linear and prominent gypsum escarpment on the southern margin (e.g., N of Canova village; Fig. 3A). In the outskirts of Sivas City, Gürsoy et al. (1992) inferred extensional neotectonics from normal faults in Quaternary terrace alluvium underlain by gypsum. Poisson et al. (2016) suggested that these structures could be related to local extension at the back of the Sivas Thrust. Most probably these local structures correspond to paleosinkholes (nontectonic structures), which are very common in the quarries excavated in Quaternary alluvium mantling evaporites, as illustrated below.

Two physiographic zones can be differentiated in the Northern Evaporitic Domain: (1) a northern ridge associated with the Sivas Thrust; and (2) a low-lying area associated with the Kızılırmak River valley, which includes the poljes analyzed in this work (Fig. 3). These two regions have been traditionally designated as the High Plateau Surface (HPS) and the Low Plateau Surface (LPS), respectively, and considered as erosional surfaces of different ages (Alagöz, 1967; Doğan and Özel, 2005; Gökkaya et al., 2021). Here, based on the clear spatial association between the northern ridge and the active Sivas Thrust, we propose that the topography is largely controlled by differential tectonic deformation and uplift controlled by a footwall ramp in the Sivas Thrust (Fig. 3B). The high-relief in the northern ridge could correspond to a hanging wall antiform (fault-bend fold) developed above the footwall ramp, that locally forces the upper evaporitic sheet to rise over a higher footwall flat. The low-lying area to the south would correspond to the trailing zone of the antiformal ridge, where the dominant plateau-like topography is largely controlled the flat geometry of the thrust. Here, fluvial and solutional erosion have a significant geomorphic imprint, mainly expressed by the Kızılırmak River valley and the gypsum poljes.

Differential uplift in the Northern Evaporitic Domain related to the thrust geometry is recorded by the variable position of the remnants of early Miocene marine limestones and marls of the Karacaören Fm. (Fig. 3). The base of this formation can be found in the High Plateau Surface 300 m above its position in the Low Plateau Surface, providing a minimum measure of differential uplift. The current activity in the hanging wall antiform of the Sivas Thrust is supported by southward migration and diversion of the Acıçay River away from the ridge in Zara area, as recoded by a 5 km long abandoned valley (wind gap) with S-stepping terraces perched ca. 100 m above the current valley floor (Gökkaya et al., 2021). The path of the W-flowing Kızılırmak River, that drains longitudinally the Northern Evaporitic Domain south of the northern ridge, is most probably controlled by lower uplift along the trailing zone of the growing antiformal ridge, confining the fluvial system along a structural through. The two structural zones in the NED display markedly different karst features (Doğan and Özel, 2005; Doğan and Yeşilyurt, 2019; Gökkaya et al., 2021; Poyraz et al., 2021). The High Plateau Surface at 1620–1500 m a.s.l. (antiformal ridge), which functions as a recharge area for the evaporite karst system, is dominated by densely packed solution sinkholes forming a remarkable polygonal karst landscape. The Low Plateau Surface (1320 and 1485 m a.s.l.) and the allogenic Kızılırmak River valley, which is the base level of the karst system, display bedrock collapse sinkholes, relict valleys, and poljes. At the Söğütlühan gauging station of the Kızılırmak River, located 18 km west of Sivas and with a catchment area of 6608 km^2, the average annual discharge for the period 1963–2004 was 38 m^3/s. The lowest discharge values are recorded in summer, and the highest flow rates occur in spring, with frequent peak values above 400 m^3/s (589 m^3/s maximum of the period). The area is characterized by continental climate with an average annual temperature of 9 °C and a mean annual precipitation of around 436 mm, largely concentrated in spring.

3. Methodology

The characteristics of the poljes and their geomorphic setting have been analyzed on the basis of detailed geomorphic mapping and field surveys. We have produced geomorphological maps using a digital surface model with a spatial resolution of 5 m resolution (Turkish General Directorate of Mapping), derived hillshades, multiple sets of georeferenced orthophotos (1966, 1973, 2015), and Google Earth historical imagery. Using these data, we have identified (1) landforms such as river terraces and relict valleys that shed light into the origin of the poljes, (2) sectors at the edges of the poljes affected by solutional undercutting and planation, and (3) hydrogeologic features such as ephemeral lakes, springs and ponors. Preliminary maps were subsequently checked and refined by field surveys, which included the examination of the known caves. Quantitative parameters were extracted with a GIS environment (i.e. ArcMap) for the morphometric characterization and analysis of the poljes. In addition, a 25-m-deep borehole (destructive drilling) was performed in bottom of Mağara Polje to obtain data on the cover deposits.

4. The gypsum poljes

4.1. General characteristics of the poljes

A total of thirteen poljes have been mapped in the central sector of the Sivas gypsum karst. These depressions form a 38 km long and ENE-WSW-oriented belt spatially associated with the Kızılırmak River valley and the morpho-structural trough situated south of the antiformal gypsum ridge at the frontal zone of the Sivas Thrust (Fig. 3). The Kızılırmak River valley displays an overall asymmetric configuration, with a rather abrupt and linear northern margin (backslope of the antiformal ridge), and a more subdued and discontinuous southern margin carved by relict valleys with a dominant NW-SE trend (Gökkaya et al., 2021). Nine poljes out of thirteen occur south of the Kızılırmak River, and five of them in the band between this main drainage and its tributary the Acısu River (Fig. 3A). The area of the poljes, ranging between 1 and 10 km^2, reaches an aggregate value of 57 km^2. They occupy 27 % of the area considering the extent of the minimum bounding polygon that encloses all the depressions (211 km^2). This high spatial density indicates the essential morphogenetic role played by the polje formative processes in this localized sector of the Sivas gypsum karst. The poljes have lengths (major axes) between 1.4 and 6 km, and mostly display an elongated plan geometry, with elongation ratios (length/width) ranging between 1.1 and 2.6 (Table 1). Nine out of thirteen depressions have elongation ratios $\geq$1.4. Unlike many other karst regions (Ford and Williams, 2007; De Waele and Gutiérrez, 2022), the orientation of the major axes shows considerable dispersion, with a weak WNW to NW prevalent trend (Fig. 3A). The plan shape geometry of the poljes is highly variable, ranging from simple polygons with linear boundaries to complex forms with highly sinuous edges displaying embayments or linear extensions. This feature is reflected by the high range of sinuosity indexes between 1.07 (Çetme Polje) and 1.80 (Tödürge Polje), given by the ratio between the perimeter of the polje and the perimeter of a circle with an area equal to that of the polje (Table 1) (Panno and Luman, 2018; De Waele and Gutiérrez, 2022).

The analyzed gypsum poljes are characterized by extremely flat floors underlain by mud-rich deposits and locally interrupted by cover subsidence sinkholes related to collapse, suffusion or sagging processes (e.g., Mağara, Çimenyenice, Sakşakkaya; Odunik) (Gutiérrez et al., 2008b; Gutiérrez, 2016). The floor of the depressions, locally lying below the floodplain of the Kızılırmak River, is situated within the water table oscillation zone (epiphreatic zone). All the depressions host lakes, either ephemeral, or permanent like the Hafik and Tödürge poljes (Figs. 4, 5, 6). Eight poljes display open margins associated with the Kızılırmak or Acısu river, showing an ill-defined boundary between the polje floor and the floodplain. These poljes can be classified as semi-closed poljes, in as much as they include internally drained area situated below the adjacent valleys, but can exchange surface water bidirectionally with the associated fluvial systems. Poljes can be affected by

Table 1
Type, morphometric parameters and some features of the mapped poljes. Genetic type: Va: Abandoned valley; Vr: Relict valley; Sc: Sinkhole coalescence. Er: Elongation ratio (L/W); Or: Orientation of major axis; Emb: Minimum elevation of polje floor; Ebl: Elevation of the base level adjacent to the polje; D: Depth of the depression, given by the elevation difference between the highest point topographic divide of the polje and Emb; Si: Sinuosity index; Lake, E: Ephemeral; P: Permanent; Topography, C: Closed; SC: Semi-closed.

Name	Genetic type	Area (km^2)	Length (km)	Width (km)	Perimeter (km)	Er	Or	Emb (m)	Ebl (m)	D (m)	Si	Lake	Topography
Dışkapı	Va	6.40	3.97	2.25	10.76	1.76	48	1283	1284	83	1.20	E	C
Odunik	Va	3.77	3.10	1.96	9.18	1.58	124	1285	1286	88	1.33	E	C
Avutmuş	Vr	2.04	2.10	1.43	5.83	1.47	151	1285	1289	60	1.15	E	C
Büyükçayır	Vr	8.28	6.00	2.28	14.50	2.64	93	1282	1283	54	1.42	E	SC
Çimenyenice	Vr	3.54	2.66	1.93	8.32	1.38	107	1290	1295	71	1.25	E	C
Çukurçayır	Vr	7.01	3.81	2.67	10.69	1.43	24	1274	1274	79	1.14	E	SC
Kulakdüzü	Vr	1.67	2.10	1.24	5.15	1.70	118	1289	1291	48	1.12	E	C
Mağara	Vr	5.13	3.16	2.14	9.10	1.48	144	1282	1288	96	1.13	E	C
Sakşakkaya	Vr	0.98	1.43	1.03	4.27	1.38	131	1291	1299	34	1.22	E	C
Lota	Vr (SC)	2.02	2.17	1.61	7.34	1.34	170	1245	1285	55	1.46	E	SC
Çetme	Sc	1.55	1.54	1.38	4.71	1.12	15	1278	1278	54	1.07	E	C
Hafik	Sc	4.76	3.33	2.62	10.83	1.27	42	1285	1289	105	1.40	P	SC
Tödürge	Sc	9.92	5.25	3.36	20.06	1.56	118	1269	1302	80	1.80	P	SC

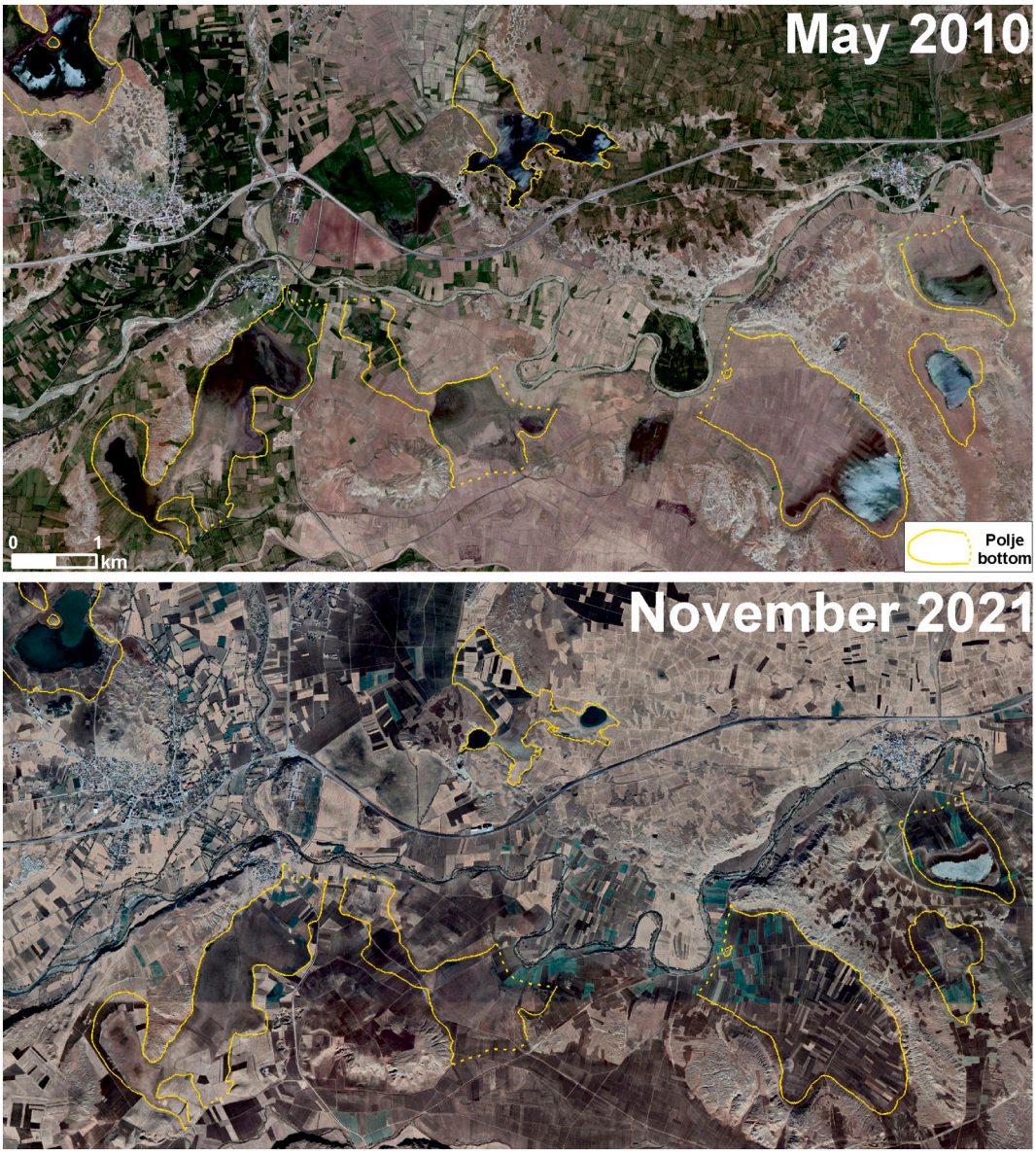

Fig. 4. Satellite images from different dates showing the development of ephemeral lakes by groundwater flooding in the floor of poljes (Google, 2022: Maxar Technologies; Airbus). Note that the water appears mostly black, but some is white due to sunlight reflections.

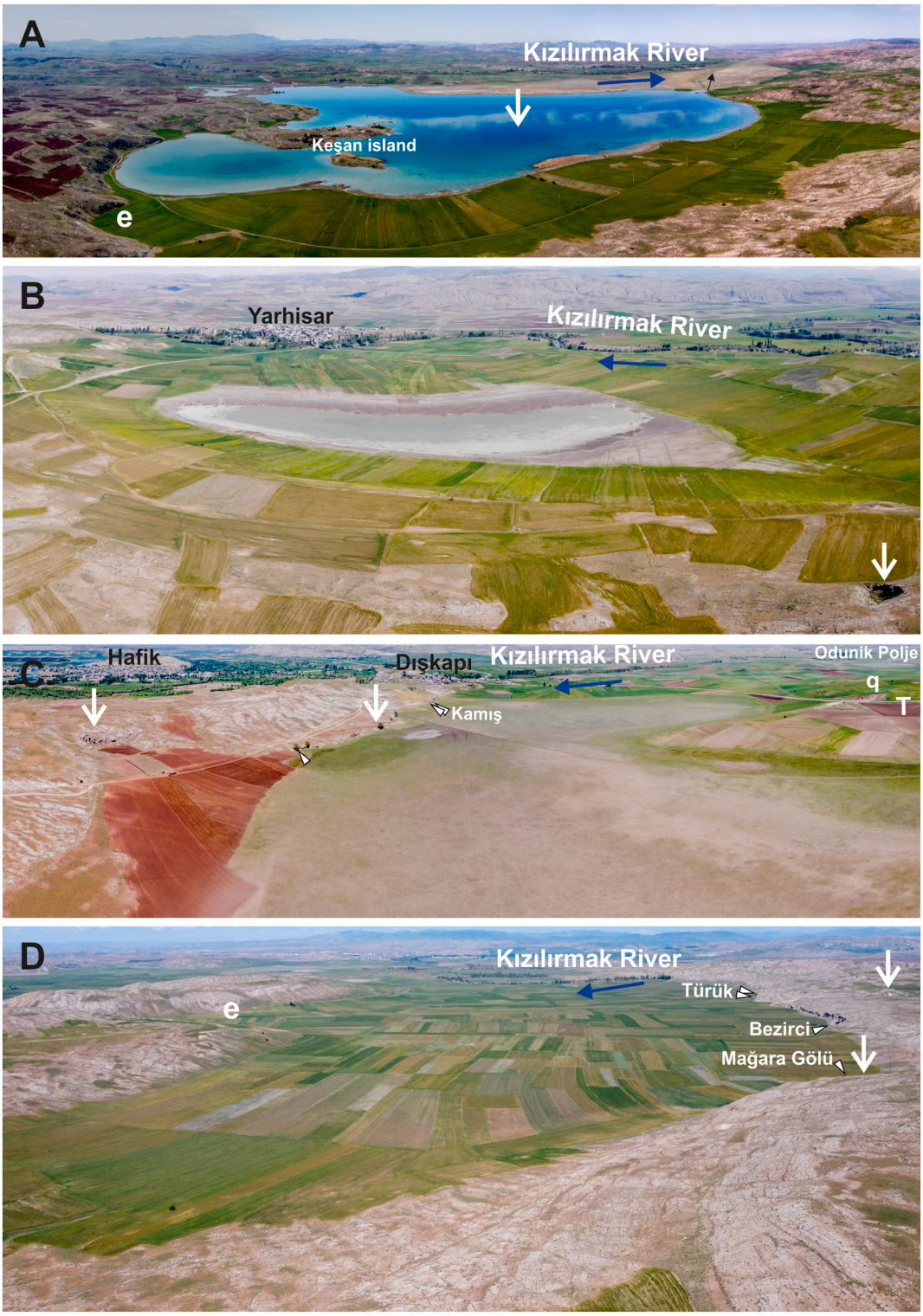

Fig. 5. Drone images of poljes. Kızılırmak River in the background. White arrows point to bedrock collapse sinkhole. White triangles indicate location of ponors or/and cave entrances. A: Tödürge Polje with the permanent Tödürge Lake. White arrows in the lake point to nested collapse sinkholes, recognisable by a darker tone. Note the embayment (e) related to the incorporation of a former sinkhole. Black arrow in the background points to artificial drainage channel. B: Kulakdüzü Polje with an ephemeral lake. Note that the floor of this open polje connects with the floodplain of the Kızılırmak River. C: Dışkapı Polje developed in an abandoned valley reach, and the terrace (T) of the pre-existing drainage with an aggregate quarry (labelled with q). The floor of this semi-closed polje merges with the floodplain of the Kızılırmak River. Odunik Polje in the background. D: Mağara Polje showing a scarped edge on the right with floodwater footcaves and ponors.

Fig. 6. Panoramic ground views of poljes of the three different types. A: Mağara Polje associated with a relict valley (left). Note bedrock collapse sinkhole (s) at the margin and embayment (e) related to the incorporation of a former sinkhole. Kızılırmak River valley (K) in the background. B: Büyükçayır Polje developed at the mouth of several transverse relict valleys. Acısu River to the left. C: Çimenyenice Polje with an ephemeral lake (el) and connected to the Kızılırmak River valley (K) in the background. D: Dışkapı Polje developed in an abandoned valley and connected to the Kızılırmak (K) and Acısu river (A) valleys. Note ephemeral lake (el) in large embayment to the left. Location of quarry in terrace deposits labelled with (q). E: Odunik Polje with ephemeral lake (el) and a ponor (p) at the foot of an arcuate scarp on the lake edge. F: Linear projection on the southern sector of Tödürge Polje with ephemeral lakes related to the coalescence of bedrock collapse sinkholes.

two types of flooding: (1) groundwater flooding by water table rise (Fig. 4); and (2) surface water flooding during floods of the allogenic Kızılırmak River, in which the water flow penetrates into adjacent depressions. These depressions also receive water input from direct precipitation, runoff derived from their restricted surface catchment, and springs of limited discharge.

The margins of the poljes display either gentle graded slopes or scarped slopes with convex-vertical profiles (Figs. 5, 6, 7). The former occurs in both gypsum and argillaceous bedrock and often grade into low-gradient aprons of fine-grained sheetwash deposits. The scarped slopes are always associated with gypsum and places where flood or lake waters interact with the bedrock causing solutional undercutting (Figs. 6, 7). The undermined slopes experience retreat mainly by rock falls and topples, producing accumulations of gypsum blocks that are rapidly worn by dissolution (Fig. 7). The rapid slope retreat by the combined effect of basal solutional undercutting and mass wasting processes results in transient slope profiles with an upper convex section and a lower vertical cliff, both separated by a sharp slope break (Figs. 7, 8). The upper gentle section typically displays a well-developed regolith and perched gullies, indicating that the scarp retreat exceeds their capacity to maintain the equilibrium profile (Fig. 7A, B; 8). The lower scarped section generally shows a sharp junction with the polje floor, a fresh appearance with abundant rock-fall scars and widespread dissolution features at the foot, including ponors, some of which correspond to small floodwater footcaves (Fig. 7). The ponors act as the main water outlet features, although subsurface drainage routes toward the regional base level (i.e. allogenic rivers) are not known. Some of the ponors might also function as springs (i.e., estavelles) during the rising stages of floods in the Kızılırmak River, that may transfer floodwater from the valley into the adjacent depressions via underground flow paths.

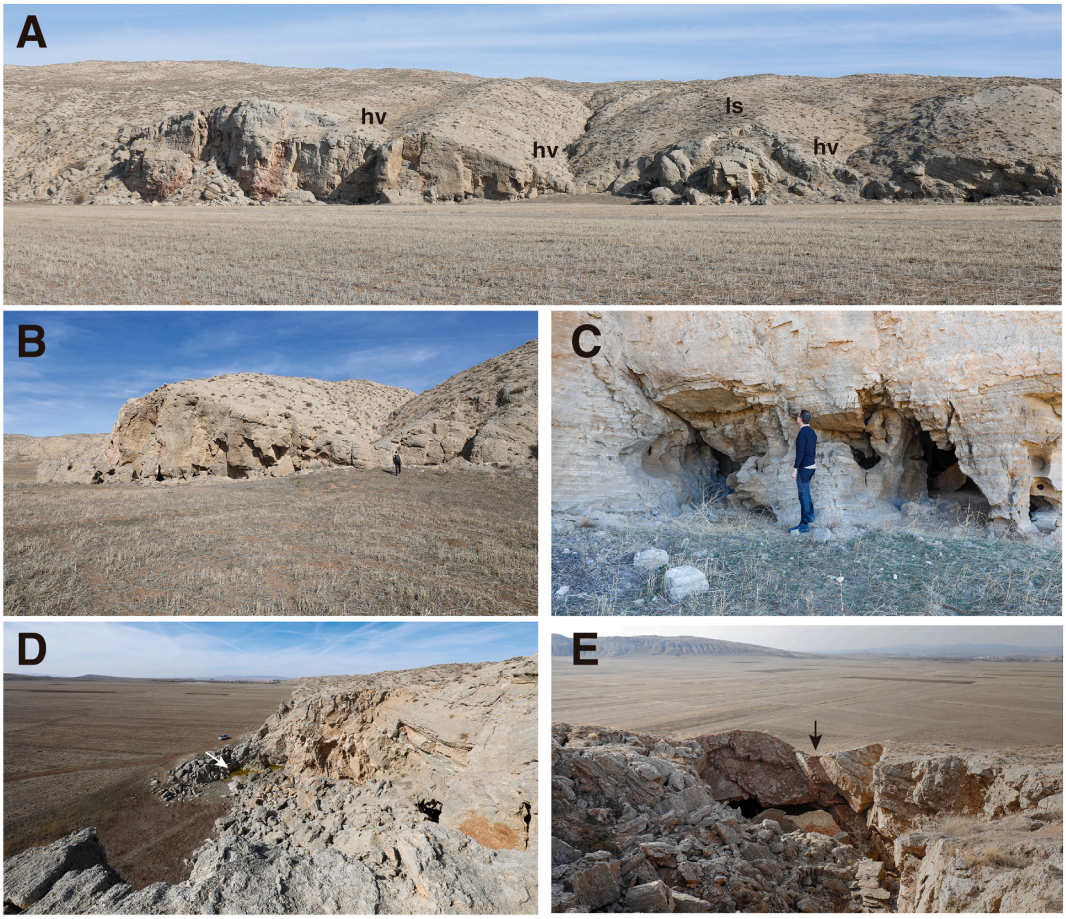

Fig. 7. Images of the scarped NE margin of Mağara Polje. A: Gypsum scarp with hanging valleys (hv), rock falls and a recent landslide expressed by an arcuate scar (ls). B: Close up view of the hanging valley at the center of fig. A. Note sharp break on the slope at the crest of the scarp and rock falls accumulated on the polje floor. C: Entrances of Türük floodwater cave largely controlled by joints within the epiphreatic zone at the foot of the scarp (footcave). D: Bezirci Ponor (arrow) with a surface water body attributable to the water table, situated a few decimeters below the polje floor. Note fresh rock fall occurred between 1966 and 1973 (comparison of aerial photographs) in the cliff undermined by solutional undercutting. E: Bedrock collapse sinkhole related to the foundering of the cave associated with Mağara Gölü Ponor. Note natural bridge with wind gap (arrow) and boulder-rich breccia related to the collapse of the cave roof.

The marginal slopes of some poljes are punctured by large bedrock collapse sinkholes (e.g., Mağara, Dışkapı, Lota, Sakşakkaya, Tödürge) that may be spatially associated with ponors and footcaves. Some of these sinkholes have disrupted drainages, expressed as perched and beheaded gullies and wind gaps (Fig. 8). Signs of instability are abundant at the margins of the sinkholes and the associated footcaves, including fresh slope movements and breakdown breccias (Figs. 7, 8). These rock collapse processes tend to reduce the bridge or threshold between the sinkholes and the poljes. Eventually, these marginal sinkholes can be incorporated into the polje depression by sinkhole and polje expansion, plus cave-roof collapse, giving place to local embayments that interrupt the linear trend of the edge of some poljes (e.g., Mağara, Lota, Tödürge) (Figs. 5, 6).

Three types of poljes can be differentiated considering their morpho-hydrological characteristics and their cartographic relationship with other landforms into three types: (1) poljes associated with relict valleys; (2) poljes developed in abandoned valley sections; and (3) poljes related to the coalescence of bedrock collapse sinkholes.

4.2. Poljes associated with relict valleys

The gypsum outcrops south of the northern antiformal ridge often display broad low-gradient relict valleys. These are remnants of an ancient drainage network largely disrupted by karst depressions such as bedrock collapse sinkholes and poljes. They mainly occur between the Kızılırmak and the Acısu rivers, showing a pervasive NW-SE trend and linearity, suggesting some structural control (e.g., fracture set) (Gökkaya et al., 2021). Their gradient and the forking orientation allow determining whether they were tributaries of the Kızılırmak or the Acısu river. Eight out of the thirteen mapped poljes occur associated with the lower reach of relict valleys (Table 1; Figs. 6, 9). The floor of the relict valleys shows a clear longitudinal inclination that attains a nearly horizontal attitude at the edge of the polje floor. Springs may occur at this slope break zones (e.g., Büyükçayır Polje). These poljes, largely related to the planation and widening of the lower section of NW-SE-oriented relict valleys, typically display an orientation consistent with that of the associated valley (i.e., inheritance). However, some poljes occur at the mouth of several relict valleys, showing a roughly transverse orientation (e.g., Büyükçayır, Çimenyenice) and suggesting the coalescence of several depressions (Figs. 3, 9). Overall, the poljes associated with relict valleys show high elongation ratios, with the highest value of 2.64 corresponding the Büyükçayır Polje, and moderate sinuosity indexes ($\leq$1.4) reflecting their relatively simple outline (Table 1).

The floor of four poljes associated with relict valleys is connected with the floodplain of the Kızılırmak River (Mağara, Kulakdüzü, Çimenyenice, Sakşakkaya; Fig. 9). However, the deepest parts of these depressions lie at lower elevation than the Kızılırmak River (see elevation differences in Table 1). Interestingly, these poljes tend to have their lowest areas and their ephemeral lakes on the opposite SE sector of the depression (Figs. 4, 9). Consequently, these poljes can be considered as

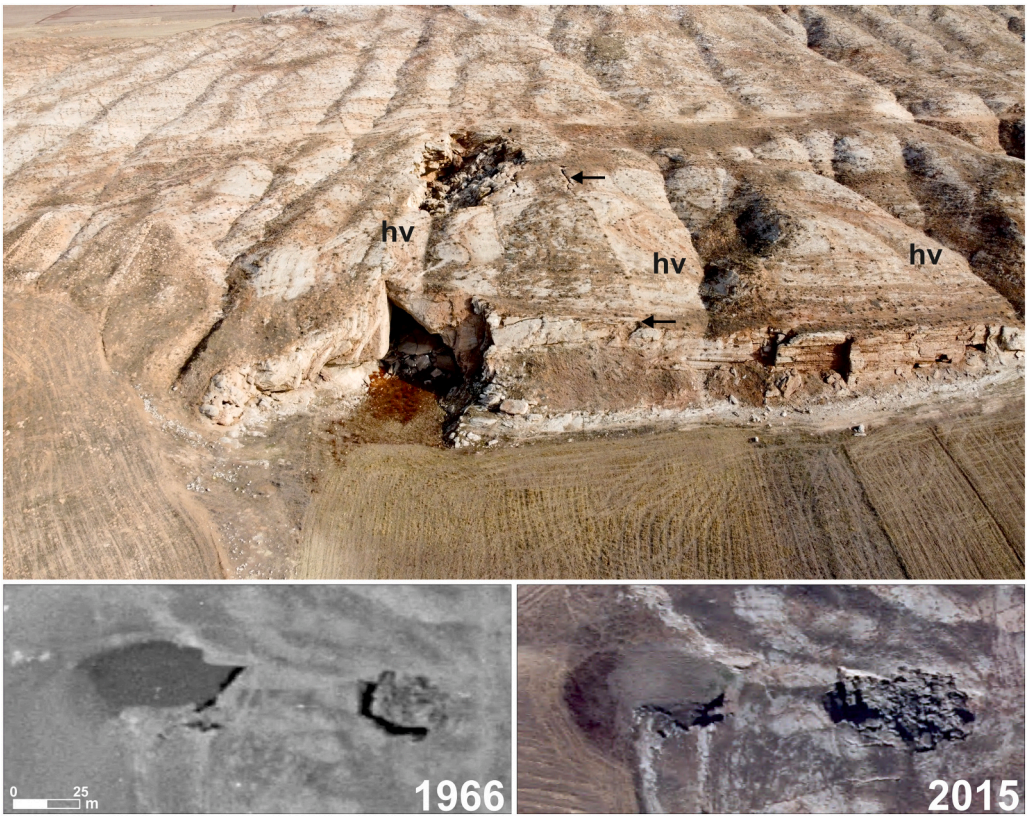

Fig. 8. Drone images of the Mağara Gölü ponor and cave at the scarped NE margin of the Mağara Polje with hanging valleys (hv) and rock falls. The west portion of the sinkhole collapsed between 1966 and 2015. Arrow points to wide open fissure controlled by tectonic fracture. The sinkhole will be eventually incorporated into the polje forming an embayment at its edge.

Fig. 9. Map on a shaded relief model with a draped orthoimage illustrating the distribution of the poljes and relict valleys in Yarhisar area. Dashed black lines indicate the ill-defined border between the polje floor and Kızılırmak River floodplain. Inset stratigraphic section indicates the texture of cover deposits drilled in Mağara Polje. Note the hum (labelled with H) located in the northwest sector of the Mağara Polje.

semi-closed depressions with internally drained areas that can receive significant water input form the adjacent allogenic river during flood events. For instance, the floor of the Mağara and Çimenyenice poljes at their SW sector are situated 6 and 5 m below the Kızılırmak River, respectively (Table 1).

The NW-SE oriented Mağara Polje, located at the confluence zone between the Kızılırmak and the Acısu Rivers, and with its floor connected with the floodplain of the former drainage, is good example of a polje developed at the mouth area of a relict valley (Figs. 5D, 6A, 9). This polje displays gentle slopes on the SW side and a scarped NE margin with hanging valleys and numerous rock falls, indicating that polje expansion is currently active along that side of the depression (Figs. 7, 8). The scarped margin displays abundant evidence of solutional undercutting along its foot and locally shows ponors, some of them connected with accessible caves, described below. Flooding events mainly affect the lowest SE sector of the polje floor (Fig. 4). Mağara ponor at the margin of

the ephemeral lake is probably the main swallow hole that drains the polje (Fig. 8), although the water can flow underground through multiple solutional conduits opened along the NE edge of the polje. This margin of the polje also displays three bedrock collapse sinkholes (Fig. 9), including Mağara Gölü sinkhole, related to the collapse of a cave associated with the ponor, and Bezirci ponor, which is the lowest point of the depression that commonly displays a water-table pond. The SW side of the polje displays a large embayment with an area of around 400 m^2, which most probably corresponds to an old bedrock collapse sinkhole merged with the polje (Figs. 5D, 6A, 9). A borehole drilled for this project in the southeast-central sector of the polje floor penetrated from top to base: (1) 11 m of massive silt and clay with secondary calcium carbonate interpreted a detrital cover; and (2) a clay-rich dissolution residue >14 m thick with increasing gypsum fragments toward the floor (Fig. 9). Hard unweathered bedrock was not reach in this drillhole. The floor of the polje contains at least three cover subsidence sinkholes (Fig. 9). The easternmost one is a cover collapse sinkhole 9 m across formed between 1973 and 2015. The flat floor of the polje is interrupted in the northwest sector by an inlier of highly karstified and undercut gypsum (residual hill), corresponding to a hum (Fig. 9).

The Lota Polje is a NW-SE oriented depression located on the northern margin of the Kızılırmak River valley. This polje shows an irregular outline (sinuosity index 1.46) on its SE sector, with projections, nested collapse sinkholes hosting permanent lakes, and undermined scarped edges with fresh slope movements. This polje shows an intermediate situation between those associated with relict valleys and those related to the coalescence of sinkholes. According to Alagöz (1967), the western and eastern sinkhole lakes reach depths of 8 and 35 m during low water table periods, respectively. During high water table periods great part of the polje becomes flooded and the lakes merge (Fig. 4). The western sinkhole, connected to the floodplain of the Kızılırmak River via a partially collapsed NNE-oriented cave, functions as the main outlet for the polje. The water emerges at a spring at the margin of a low-lying swampy area in the floodplain of the Kızılırmak River, and is drained by an artificial channel.

4.3. Poljes developed in abandoned valley sections

The Dışkapı and Odunik poljes occur between the W-flowing Kızılırmak and Acısu rivers, situated around 3 km apart (Fig. 10). Dışkapı Polje has a NE-SW orientation, whereas Odunik Polje has a NW-SE elongation trend. Between the two poljes there is a gypsum relief largely mantled by gravelly terraces with degraded surfaces and largely disconnected from the current drainages. Six terrace levels ascribable to the Acısu River have been differentiated on the basis of their relative height (Ta1: +73 m; Ta2: +67 m; Ta3: +53 m; Ta4: +34 m; Ta5: +20 m; Ta6: +9 m). These terraces, particularly Ta4 and Ta5, display an arcuate distribution about the highest sector of the relief (Ta1, Ta2, Ta3). These cartographic relationships record a former valley section of the Acısu River, that used to form an open bend. Eventually, the incised valley meander was cut off and the poljes developed in the two abandoned arms of the valley meander. North of Odunik polje there are N-stepping terraces of the Kızılırmak River (Tk1: +42 m; Tk2: +39 m; Tk3: +20). The distribution of the terraces and the present-day river channels suggest that the change in the path of the Acısu valley occurred sometime after the formation of terrace Ta6 and when the Kızılırmak River was situated in a more northern position, as supports the large embayment located E of Hafik. The abandonment of the valley section is also supported by the presence of fluvial gravel below the floor of Dışkapı Polje (Fig. 10).

The NE-SW oriented Dışkapı Polje shows a large subcircular embayment with an ephemeral lake on its SW sector attributable to the incorporation of a former single or compound bedrock collapse sinkhole into the polje. The polje floor, although locally situated below the floodplains of the Kızılırmak and Acısu rivers (Table 1), connects with them on both extremes of the depression. The polje has a rather sinuous SE edge with gentle slopes associated with the alluvium-mantled relief. In contrast, the NW edge is mostly defined by a linear gypsum scarp with multiple evidence of solutional undercutting, rock falls, ponors and floodwater footcaves (e.g., Kamış Cave). This polje can experience flooding by water table rise (Fig. 4) and by the incorporation of floodwater from the adjacent Kızılırmak and Acısu rivers. During flood recession, the polje is mainly drained underground toward the Kızılırmak River by the ponors and caves located along its NW margin. A borehole drilled in floor of the polje by the State Hydraulic Works (DSİ) (see location and simplified log in Fig. 10) penetrated 30 m of unconsolidated deposits without reaching the bedrock. The lower section, 14 m thick, is dominated by fluvial gravels, whereas the upper 6 m mainly consist of fine-grained facies. The anomalously high thickness of the cover is probably related to synsedimentary subsidence due to gypsum dissolution, or the presence of alluvium-filled palaeosinkholes (Gutiérrez and Cooper, 2013 and references therein). Odunik Polje displays three nested ephemeral lakes and its floor is also connected to the floodplains of the adjacent drainages. A ponor occurs at the foot of an arcuate gypsum scarp on the SW edge of the central ephemeral lake. On its NE side, the extent of the polje has been reduced by the SW migration

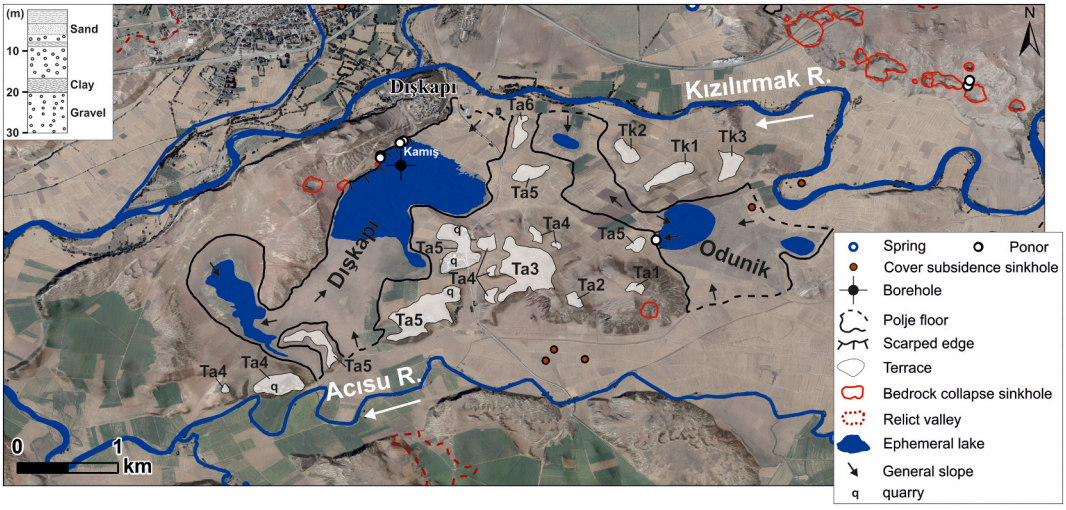

Fig. 10. Map on a shaded relief model with a draped orthoimage showing Dışkapı and Odunik poljes, both developed in abandoned valley section of the Acısu River. The terraces of the Acısu River (Ta4 and Ta5) allow inferring former valley meander currently occupied by poljes. Dashed lines indicate the ill-defined boundary between the polje floor and floodplains of the adjacent rivers. Inset stratigraphic section indicates the texture of cover deposits logged in Dışkapı Polje.

of a meander loop of the Kızılırmak River.

Quarries excavated in some terraces situated at the margins of Dışkapı Polje (Fig. 10) display striking examples of paleosinkholes. The fluvial deposits mainly consist of gravels with intercalations of tabular beds of fine-grained facies that constitute valuable markers for the characterization of the deformation. The subsidence structures are mostly cover collapse paleosinkholes bounded by well-defined collapse faults, and in some cases can be described as cover collapse and sagging paleosinkholes, with significant downward bending in the down dropped sediments, including coffer-like and sheath folds (Fig. 11). The collapse faults are expressed as well-defined shear zones with reoriented fabrics and hardened by the accumulation of secondary carbonate. The beds associated with these failure planes typically display high amplitude drag folds, most probably developed in soft sediment soon after their deposition. The collapse normal faults can display variable attitudes; vertical, inward-dipping, and outward-dipping (pseudo-reverse faults). Inward dipping faults may correspond to funnel-shaped failures, in which the collapsing sediments penetrate through a progressively smaller section. This space problem can lead to the development of sheath folds with significant internal deformation and/or conjugate systems of splaying over-steepened normal faults.

The down dropped sediments in a funnel-shaped collapse include massive structureless silts and sands with gravel pockets tens of centimetres across (Fig. 11). The development of this type of soft-sediment deformation structures associated with paleosinkholes has been explained by sudden collapses affecting soft water-saturated deposits. The dynamic loading associated with the rapid collapse results in pore-fluid overpressure conditions and the liquefaction of the deposit. This liquefaction process leads to the obliteration of the internal structure of the sediments and the downward segregation (elutriation) of the heavier gravels, ultimately forming pockets embedded into fine-grained material (Gutiérrez, 1998, 2014; Guerrero et al., 2008). Similar structures found in other sedimentary environments (e.g., fan delta, fluvial, pyroclastic surge) have been interpreted by several authors as liquefaction-fluidization features (Postma, 1983; Johnson, 1986; Nocita, 1988).

Similar normal faults were documented by Gürsoy et al. (1992) in terrace deposits of the Kızılırmak River underlain by gypsum in Sivas city area. These authors ascribed them to active extensional faulting, despite the region is subject by a compressional tectonic regime. They also indicated that the formation of a few associated reverse faults records a different tectonic phase. Poisson et al. (2016) suggested that they could record active extension at the back of the Sivas Thrust. Most probably those structures also correspond to paleosinkholes related to the dissolution of the evaporitic bedrock. A number of criteria support the gravitational (non-tectonic) origin of the Quaternary deformations observed in the quarries located in the vicinity of Dışkapı Polje (e.g., De Waele and Gutiérrez, 2022): (1) the paleosinkholes do not show any significant vertical offset across the collapse blocks (i.e., stratigraphic markers at similar elevation on both sides); (2) some outcrops clearly show that the failure planes have a funnel-shaped or cylindrical geometry (ring faulting); (3) the deformations are widespread and show a local extent, and cannot be related to mappable faults with geomorphic expression; and (4) the strain mainly occurred during and soon after the deposition of the terraces, before they became relict morpho-stratigraphic units perched above the base level, indicating that hydrogeological conditions (i.e., dissolution) controlled the timing of the deformations.

4.4. Poljes related to sinkhole coalescence

The Hafik and Tödürge poljes are located north of the Kızılırmak River, at the foot of the backslope of the antiformal gypsum ridge (Fig. 3). Both are characterized by a complex geometry in plan with high sinuosity indexes of 1.4 and 1.8, respectively (Table 1), and the presence of large permanent lakes with significant depths. Tödürge Polje, covering 9.9 km^2 is the biggest polje and hosts Tödürge Lake, which is one of the largest karst lakes in Turkey, with an area of 3.3 km^2 (Figs. 5A, 12). This water-table lake receives calcium sulphate water from springs located in Silgin depression, which is an elongated compound sinkhole connected to the polje and resulting from the merging of at least four bedrock collapse sinkholes (Gökkaya et al., 2021). The Tödürge Lake used to drain eastward into a large backswamp situated at the margin of the floodplain of the Kızılırmak River, but currently it is connected to the Kızılırmak River at Yarhisar village via an artificial canal 9 km long. The eastern side of the polje displays several embayments related to the coalescence of former adjoining bedrock collapse depressions with the polje. Some of them are inundated by Tödürge Lake, whereas others contain disconnected lakes. Bathymetric data provided by Alagöz

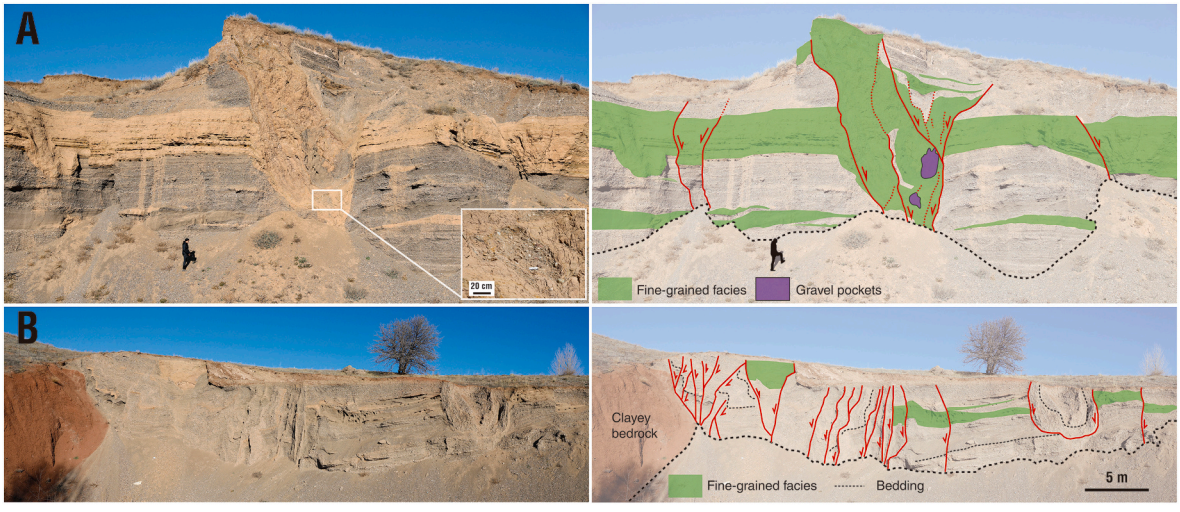

Fig. 11. Paleosinkholes exposed in quarries excavated in terrace deposits of the Acısu River associated with the Dışkapı Polje. A: Cover collapse paleosinkhole bounded by inward dipping faults. The foundered deposits include structureless fine-grained facies with embedded gravel pockets (inset image) attributable to liquefaction and elutriation induced by a sudden collapse. B: Two collapse paleosinkholes with contrasting structural features. The one on the left, abutting clayey bedrock, shows an asymmetric geometry with a dense network of subvertical failure planes on the right, and inward dipping faults with splaying pseudo-reverse secondary faults. The asymmetry of the sinkholes is probably related to dissolution of gypsum at the contact with impervious argillaceous bedrock (contact karst). The small collapse on the right corresponds to the section of a small collapse bounded by an inclined cylindrical or funnel-shaped fault. The down dropped sediments display a sheath fold most probably developed when the deposit was in a soft and water-saturated state.

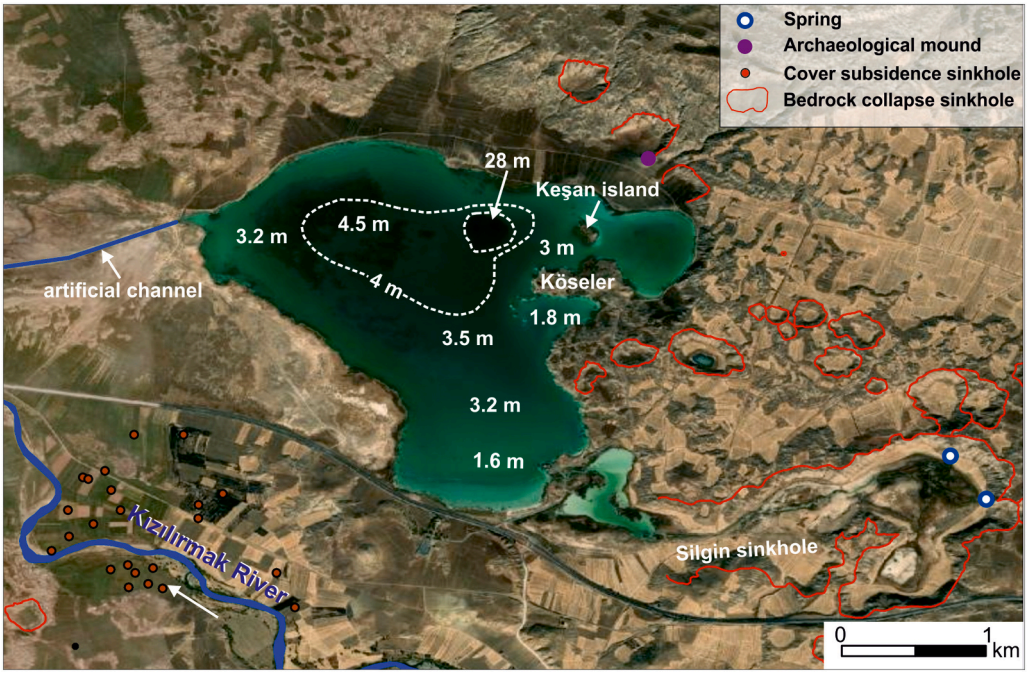

Fig. 12. Annotated satellite image of the Tödürge depression indicating bathymetric data from Alagöz (1967), and a nested submerged collapse sinkhole 28 m deep (Sources: Esri, DigitalGlobe, GeoEye, i-cubed, USDA FSA, USGS, AEX, Getmapping, Aerogrid, IGN, IGP, swisstopo, and the GIS User Community). Note multiple embayments on the eastern side of the lake and the polje related to the coalescence of former bedrock collapse sinkholes with the expanding polje.

(1967) indicate that most of the lake has a depth of <4 m, but its relatively flat floor is interrupted west of Keşan Island by a nested collapse sinkhole 28 m deep and around 220 m across. Both, the geometry of the lake bottom and the morphology of the polje edge, with several rounded sections, indicate that this large karst depression is largely related to the coalescence of multiple bedrock collapse sinkholes. Similarly, the Hafik Polje with area 4.8 km^2 hosts a lake 2–3 m deep (Alagöz, 1967) with a clover-like geometry (tri-lobate) attributable to sinkhole coalescence. Hafik Lake is also connected to the Kızılırmak River through an artificial canal starting at its NE edge. The Çetme polje on the northern margin of the Kızılırmak River valley, is also attributed to sinkhole coalescence. This polje hosts an ephemeral lake a displays degraded margins and relatively low sinuosity index of 1.46, probably reflecting its maturity.

4.5. *Floodwater footcaves*

The edges of the poljes that get in contact with floodwaters (i.e., permanent and ephemeral lakes) typically display scarped gypsum slopes with basal undercuts. The lower parts of the cliffs show abundant dissolution features such as fissures and conduits related to the solutional enlargement of discontinuity planes (Fig. 7C), and spongework resulting from the differential etching of nodular gypsum (Fig. 13A). Locally, dissolution occurring within the epiphreatic zone (i.e. water-table oscillation zone) has generated horizontal caves of limited accessible extent (e.g., NE edge of Mağara Polje and NW edge of Dışkapı Polje) (Figs. 9, 10). The patterns of these floodwater footcaves display two end members and intermediate situations between them. Some caves or cave sectors are essentially wide openings with flat solutional ceilings that split into multiple tapering dead-end passages (e.g., Kamış Cave in the Dışkapı Polje) (Fig. 13B). In other cases, the caves are small anastomotic mazes of widened fissures and conduits largely controlled by joints, and intervening residual rock pendants and walls (e.g., sections of Mağara Gölü and Türük caves in Mağara Polje) (Fig. 13C, D). The floor of the caves, generated by quasi-static floodwaters, is characterized by flat surface underlain by a veneer of fine-grained deposits (Fig. 13B, C, D, E). This basal shield prevents downward dissolution and promotes the widening of the passages by the development of solution notches. These horizontal waterline notches commonly display multiple high-water marks and can be carved by solution pockets (Fig. 13E). Locally, intersecting solution conduits and solution pockets in the walls and rock residuals produce intricate morphologies with sharp edges often known as echinoliths (Fig. 13D). Close to the cave entrances and above the elevation range of frequent inundation, the gypsum exposures, rather than showing a smooth surface, may display tightly packed centimeter-sized hollows and sharp cusps ascribable to condensation solution (Lundberg, 2019) (Fig. 13F), or a flaking and spalling weathering crust related to weathering by dissolution and re-precipitation processes.

The quasi-static condition of the floodwaters in the caves developed in the polje margins areas favor the accumulation of fine-grained deposits in their floor by decantation of suspended load. These hydrodynamic conditions explain the lack of scallops typically found in other floodwater caves with rapid flow velocities (Palmer, 2007). These gypsum caves can expand at high rates into the polje margins, but are not expected to reach significant dimensions due to simultaneous destruction in the entrance areas by slope movements and cave-roof collapse. The important role played by instability phenomena in the evolution of floodwater gypsum caves has been documented in a number of cave systems in and slope movements (Andrejchuk and Klimchouk, 2002; Sivinskih, 2009; Franz et al., 2013).

Dışkapı Polje has two cave systems between the polje floor and the Kızılırmak River, situated around 500 m apart. Kamış Cave has two nearby entrances at the foot of the gypsum cliff and the main passage is 40 m long and approximately parallel to the edge of the polje (Mayer, 1973, 1974) (Fig. 13B). Waltham (2002) noted that the cave passages must continue, though very small conduits, toward the Kızılırmak River. Mağara Gölü Cave in Mağara Polje has a large entrance carved in gypsum strata steeply dipping toward the polje (i.e. monoclinal fold) (Fig. 8). The solution notch associated with the high-water mark around 4 m shows multiple recesses and projections related to differential dissolution of the different layers. This entrance area also shows numerous solution pockets produced by floodwaters forced into penetrable discontinuities. The collapse of the cave roof has produced a bedrock collapse sinkhole 46 m long and with a NNW-SSE orientation (Fig. 8). The non-collapsed portion of the cave roof remains as a natural

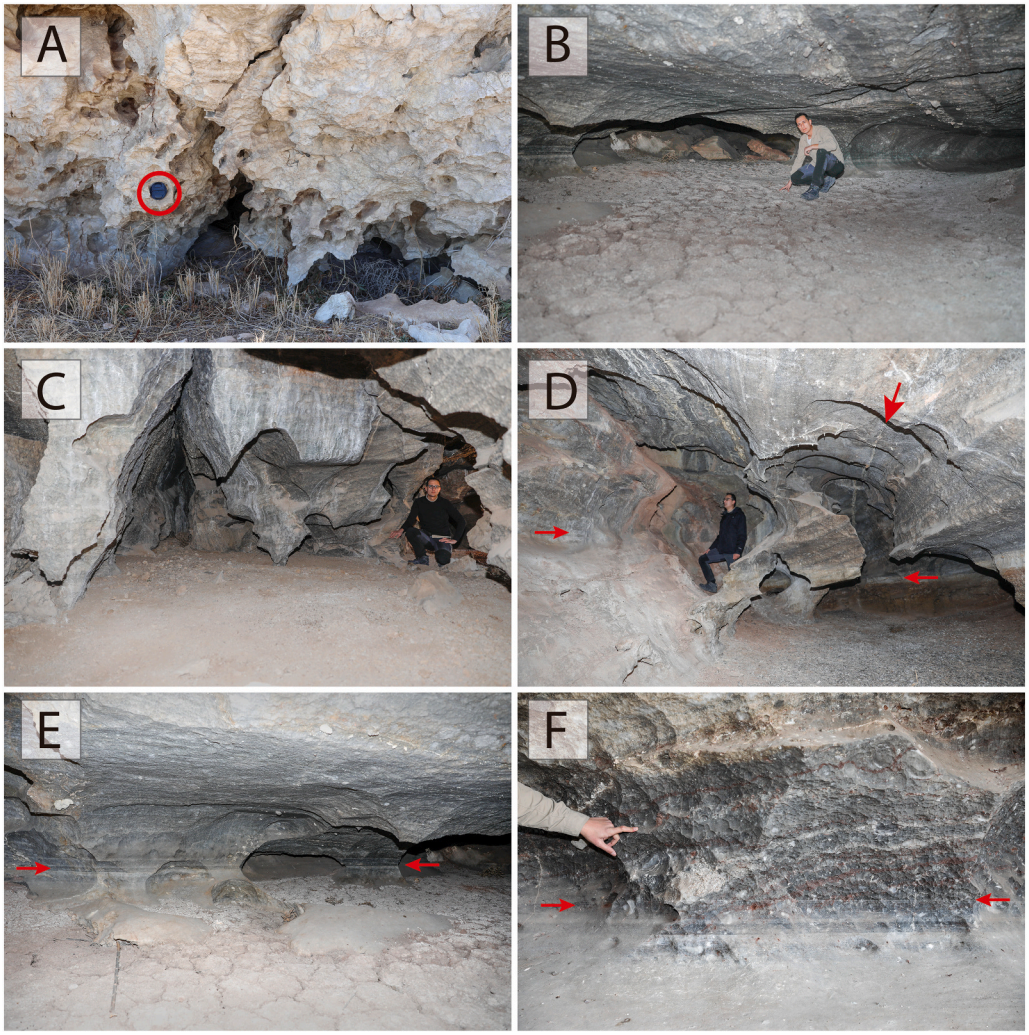

Fig. 13. Solution features and caves associated with the scarped margins of the Dışkapı and Mağara poljes. A: Spongework developed in nodular gypsum at the foot of a cliff in Dışkapı Polje. Encircled cap lens 8 cm in diameter for scale. B: Wide passage in Kamış Cave with flat solutional ceiling and flat aggraded floor that split into tapering dead-end conduits. C and D: Joint-controlled fissures and conduits and intervening rock pendants indented by intersecting solution pockets in Türük Cave and Mağara Gölü Cave. Note floor shielded by muddy deposits. Arrows in D point to perched solution notch (left), joint (up) and high-water marks (right). E: Solution notch in Kamış Cave caved by solution pockets. Arrow points to high-water mark. F: Solution hollows and cups attributable to condensation solution above high-water mark (arrows) in Kamış Cave.

bridge. The comparison of aerial photographs from different dates reveals that before 1966 the sinkhole used to have a circular geometry. However, at least two collapse events occurred between 1966 and 2015 enlarged and elongated the depression toward the polje, Eventually, further collapse processes and dissolution acting on the breakdown deposits are expected to integrate the sinkhole into the polje and transform it into an embayment. Bezirci Ponor in the Mağara Polje most probably used to be a cave that has been incorporated into the polje, showing an ephemeral lake partially surrounded on the polje side by bedrock residuals (Fig. 7D).

5. Discussion

Considering that reports on gypsum poljes are incidental (Sauro, 1996; Gutiérrez and Cooper, 2013), the Sivas poljes offer an exceptional opportunity to learn about the characteristics and associated features (e.g., caves), origin and controlling factors of these scarce and poorly known gypsum karst landforms. The thirteen poljes documented in this work are relatively small (1.4–6 km long, 1–10 km^2 in area) (Fig. 3A; Table 1), compared with the dimensions that typically show poljes in carbonate terrains, many of which reach several tens of kilometers long. Although the Sivas poljes mostly show elongated shapes, the orientations of the major axes do not show a clear prevalent trend and their margins do not display rectilinear geometries controlled by active or inactive faults (Fig. 3A), which is a common feature in many limestone poljes (border poljes, neotectonic poljes). Instead, some of the poljes show highly irregular edges as indicated by the high sinuosity indexes (Table 1). The depressions are characterized by extremely flat floors (Figs. 5, 6) underlain by a cover of fine-grained deposits (i.e., detrital, dissolution residues). The floors largely lie within the water table oscillation zone (epiphreatic zone) and are locally occupied by large ephemeral or permanent lakes (Fig. 4). A very peculiar feature of the Sivas poljes is that the floor of most of them is connected to the floodplains of the allogenic Kızılırmak and/or Acısu rivers through gaps in their topographic margins. Nonetheless, the deeper parts of the polje floors lie at lower elevation than the adjacent floodplains, functioning as semi-closed hydrological basins. The polje floors, situated within the epiphreatic zone, can be affected by two types of flooding: (1) groundwater flooding related to water table rise; and (2) surface water flooding, when floodwaters of the Kızılırmak and/or Acısu rivers penetrate into the adjacent and lower-lying basins. The margins of the poljes associated with ephemeral or permanent floodwaters typically display scarped gypsum slopes with evidence of active basal solutional undercutting (i.e., solution notches, floodwater footcaves often functioning as ponors), and evidence of rapid slope retreat related to lateral solution planation, including hanging valleys and slope movements (Fig. 7). These geomorphic and hydrological features indicate that the Sivas gypsum poljes can be classified from the genetic perspective as base-level poljes (Ford and Williams, 2007; De Waele and Gutiérrez, 2022).

The hydro-geomorphic characteristics of the poljes and the cartographic relationships with other landforms allow the differentiation of three types of base-level poljes with distinctive evolutionary styles (i.e.,

morphologic convergence or equifinality): (1) poljes associated with relict valleys; (2) poljes developed in abandoned valley sections; and (3) poljes related to the coalescence of bedrock collapse sinkholes (Fig. 14).

Eight out of the thirteen mapped poljes have been developed at the lower reaches of wide, low-gradient relict valleys (Figs. 9, 14C). These are mostly old tributary valleys of the Kızılırmak River with a prevalent NW-SE trend, most probably formed under more humid conditions in the past, that have been disrupted by the formation of poljes. These depressions, characterized by marked elongation and expressed as internally drained widenings in the lower reach of the valleys, record the progression of dissolution-induced subsidence and solution planation in two main directions: (1) upstream along the valley floor; and (2) laterally at the valley margins, eventually leading to the coalescence of poljes developed in adjacent relict valleys (e.g., Büyükçayır Polje).

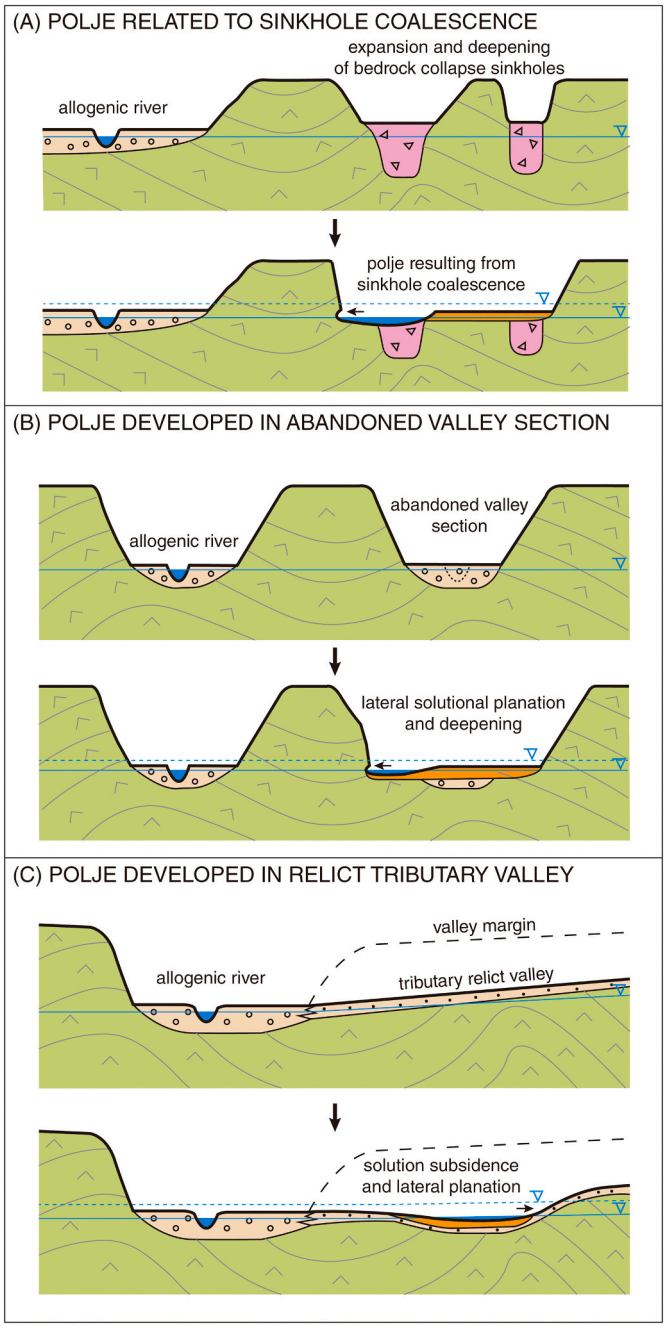

Fig. 14. Sketches illustrating different evolutionary paths resulting in the development of base-level poljes associated with major allogenic rivers in the Sivas gypsum karst. (A) The lateral growth and deepening of adjacent bedrock collapse sinkholes may result in their coalescence. Eventually, the floor of the deepening compound sinkhole may reach the epiphreatic zone, starting to behave as a base-level polje that expands by lateral solution planation. (B) Poljes may form in abandoned valley sections lying within the epiphreatic zone. Subsidence related to subsoil dissolution and lateral solution planation lead to the deepening and expansion of the depression. (C) Differential dissolution-induced subsidence creates a depression in a relict tributary valley, becoming a blind valley locally within the epiphreatic zone. The floor of the depression expands upstream and laterally by subsoil dissolution and lateral solution planation.

Terrace mapping indicates that the Dışkapı and Odunik poljes have formed in an abandoned reach of the Acısu River valley, that used to form a now cut-off open bend (Fig. 14B). This interpretation is corroborated by fluvial gravels encountered in a borehole drilled in the floor of Dışkapı Polje (Fig. 10). The abandoned valley reaches can be affected by solutional deepening, becoming internally drained depressions, plus lateral solution planation resulting in the expansion of the poljes. Some authors (e.g., Phillips, 2017) document in carbonate karst areas geomorphic evidence of fluvial-to-karst (e.g., dry valleys) and karst-to-fluvial transitions (e.g., sinkholes breached by drainages). However, to our knowledge, this is the first case study that documents an evolutionary trend involving the transformation of fluvial landforms (i.e., relict valleys, and abandoned valley sections) into gypsum poljes.

The Hafik and Tödürge poljes are the result of the amalgamation of several bedrock collapse sinkholes. These poljes are characterized by a complex geometry in plan, with large embayments, high sinuosity indexes, and the presence of permanent lakes with nested submerged sinkholes (Fig. 12), whereas the more mature and degraded Çetme polje displays a simple geometry. Gökkaya et al. (2021), based on a cartographic and morphometric analysis of the bedrock collapse sinkholes in the Sivas karst, document the significant enlargement that experience these depressions in the high-solubility gypsum bedrock, involving different modes of erosion, including solutional undercutting, slope movements, and chemical and mechanical denudation by runoff water. The interpretation of the development of poljes by the coalescence of bedrock collapse sinkholes fits with the evolutionary model proposed in the early days by Cvijić (1893, 1918), whereby dolines evolve into uvalas (compound sinkholes) and then into poljes, although this concept was largely dismissed (e.g., Sweeting, 1972).

The allogenic Kızılırmak and Acısu rivers constitute the regional base level for the Sivas gypsum karst. These fluvial systems have experienced long-term episodic downcutting as recorded by the mapped stepped fluvial terraces, most probably in response to regional uplift within an active compressional environment. The path of those major drainages in the Northern Evaporitic Domain of the tectonically inverted Sivas Basin is controlled by a structural trough, south of the antiformal ridge associated with the front of the active N-verging Sivas Thrust with a footwall ramp. The water table drops related to fluvial entrenchment episodes lead to karst rejuvenation phases, in which the denudation style is dominated by the lowering of the ground surface mainly by dissolution acting in the vadose zone. Once the topographic surface is worn down to the water table oscillation zone (epiphreatic zone), erosion mainly proceeds by slope retreat via lateral solution planation, with the progressive expansion of the base-level plains (e.g., polje floors). In the Sivas karst, both processes (solutional lowering and planation) can operate at significantly high rates given the high solubility of the gypsum bedrock and the presence of allogenic rivers that continuously supply abundant aggressive water to the karst system. Dissolution of the gypsum bedrock beneath the cover (i.e., subsoil dissolution) produces a progressively thicker residual soil (dissolution residue) and gradual subsidence in the ground surface, which can be hardly counterbalanced by aggradation in these starved topographic basins characterized by extremely flat floors. Unlike in carbonate terrains, subsoil dissolution in gypsum is not boosted by acidity enhancement of the water that percolates through CO2-rich soils (i.e., cryptocorrosion; Nicod, 1975; Fabre and Nicod, 1982; Gracia et al., 2003; Bruxelles et al., 2007), but by the

spatially continuous and prolonged water-rock interaction that occurs beneath damp soils (De Waele and Gutiérrez, 2022). However, this subsoil dissolution process acting at the rockhead can be substantially inhibited by the low permeability of the clay-rich cover that retards the renewal of aggressive water.

When the poljes become inundated, either by water table rise (groundwater flooding) or by the incorporation of floodwaters from the nearby rivers (surface water flooding), large volumes of aggressive water get in contact with the marginal gypsum slopes. A great part of the solutional work is achieved at the edges of the depressions, since the low-permeability cover of the floors prevents rapid percolation of water. The long-sustained interaction of the floodwaters with the high-solubility gypsum bedrock within the epiphreatic zone can cause widespread dissolution, like an advancing dissolution front, causing basal solutional undercutting. The floodwater is also forced into all the penetrable openings such as joints and bedding planes resulting in the development of "water-injection" solution features such as tapering dead-end fissures and solution pockets (Palmer, 1991, 2007; De Waele and Gutiérrez, 2022). Close to the retreating scarp affected by erosional unloading, these discontinuity planes have typically experienced some dilation, facilitating water flow and solutional widening. Ultimately, the different dissolution modes acting at the foot of the scarp (i.e., widespread, differential) lead to the basal notching of the slopes and the development of floodwater footcaves (Fig. 13). These epiphreatic caves may display a significant longitudinal development parallel to the scarp and anastomotic patterns related to the widening of intersecting discontinuities. The undermined gypsum slopes retreat by mass wasting processes, resulting in the expansion of the polje floors that are time transgressive surfaces progressively younger toward the margins. For this reason, poljes are remarkably wide depressions compared to their depth. The deposits derived from the slope movements, made up of high-solubility gypsum are readily removed by dissolution (Klimchouk et al., 1996; Klimchouk and Aksem, 2005; De Waele and Gutiérrez, 2022). Pechorkin (1969) estimated average surface recession rates of 79–190 mm yr^{-1} in gypsum boulders permanently in contact with water in the Kama River reservoir, Russia. James et al. (1981) calculated a retreat rate of 80–100 mm yr^{-1} for an undercut gypsum cliff in contact with the allogenic River Ure in England. The rapidity of the recession of the scarped gypsum slopes is evidenced by the presence of convex-vertical profiles and hanging valleys (Figs. 7, 8). The collapse of these caves may result in the development of bedrock collapse sinkholes at the margins of the poljes (Fig. 8), that may be ultimately integrated into the latter expressed as large embayments (Figs. 5A, D; 6A).

The development of the rare gypsum poljes in the Sivas karst seems to be related to a number of factors, as suggested by their spatial distribution concentrated along a belt (Fig. 3A) and their cartographic relationships: (1) The morpho-structural trough situated south of the frontal ridge associated with the Sivas Thrust provides an adequate hydrological and structural setting for the formation of poljes. On the one hand, it guides the path of the main drainages (Kızılırmak and Acısu rivers) that function as the base level for the karst system. On the other hand, uplift rate in this structural zone, probably dominated by horizontal translation over a thrust flat, should be low enough for the fluvial system and poljes to maintain their floors as base level plains within the epiphreatic zone. This does not seem to be the case of the northern gypsum antiformal ridge, dominated by a polygonal karst of densely packed solution sinkholes lying well above the water table. (2) The allogenic Kızılırmak and Acısu rivers continuously supply abundant aggressive water for the development and enlargement of the poljes. These fluvial systems can contribute to the flooding of the poljes by inducing water table rises during high-discharge seasons and by supplying surface water during fluvial floods. (3) The area has a fluviokarst landscape, including relict and active fluvial landforms that propitiate the initiation of poljes. Eight out of thirteen poljes have been formed in relict valleys probably formed under more humid palaeohydrological conditions, and two in abandoned sections of the Acısu River. (4) The Sivas gypsum karst shows a high frequency of large and clustered bedrock collapse sinkholes (Gökkaya et al., 2021) that may evolve into poljes by their coalescence.

6. Conclusions

The gypsum poljes mapped and characterized are an exceptional example worldwide, since these type of karst depressions are essentially found in carbonate terrains. The poljes in Sivas are concentrated along a belt associated with the regional base level (Kızılırmak and Acısu rivers) and the trailing morpho-structural trough of the frontal antiformal ridge of the active Sivas Thrust. The thirteen inventoried poljes, with their floors mostly situated within the water-table oscillation zone (i.e., epiphreatic zone), are classified as base-level poljes from the genetic perspective. A significant peculiarity of the Sivas poljes is that the floor of a significant proportion of the depressions is connected to the floodplain of the Kızılırmak and Acısu Rivers, but situated at lower elevation. Consequently, they function as semi-closed basins that may be affected by groundwater flooding (i.e., water table rise), and surface-water flooding derived from the adjacent fluvial systems. In contrast with most of the poljes described in carbonate karst settings, the gypsum poljes of Sivas, despite being located in an active compressional environment, do not show a clear structural control.

Three types of evolutionary paths have been differentiated for the base-level poljes on the basis of their characteristics and the cartographic relationships with other landforms (Fig. 14): (1) poljes initiated from relict valleys; (2) poljes developed in abandoned valley sections; and (3) poljes resulting from the coalescence of bedrock collapse sinkholes. Ten out of thirteen poljes have formed in former fluvial landforms (i.e., relict valleys, abandoned valley reaches), indicating the important role played by inheritance, past hydrological conditions and fluvial dynamics in their development.

The formation and enlargement of the poljes, with their floors situated within the epiphreatic zone, is related to lateral solution planation by lake and flood waters acting at the margins. The semi-static waters in contact with the marginal slopes cause basal solutional undercutting, mass movements that are rapidly removed by dissolution, and the consequent retreat of the slopes, generating time-transgressive base-level solution plains in the polje floors. This planation process can proceed at much higher rates than in carbonate karst terrains given the high solubility of the gypsum, as supported by the common presence of hanging valleys in the scarped margins. The floodwaters in contact with the gypsum can cause both widespread solutional undercutting along the foot of the slopes and preferential dissolution by water forced into discontinuities (e.g. joints, bedding), eventually resulting in the development of subhorizontal floodwater footcaves that may function as ponors. Bedrock collapse sinkholes generated by the foundering of the cave roofs can be incorporated into the poljes, generating embayments at the margins.

The main factors involved in the development of gypsum poljes in Sivas include: (1) a favorable structural setting within a compressional tectonic environment, given by a morphostructural trough with relatively low uplift rate that control the path of two major drainages; (2) continuous supply of abundant aggressive water from the allogenic Kızılırmak and Acısu rivers; (3) the presence of a fluviokarst landscape with fluvial landforms that can be transformed into karst depressions; and (4) clusters of bedrock collapse sinkholes that experience rapid enlargement and eventually coalescence.

Declaration of competing interest

We wish to confirm that there are no conflicts of interest associated with this publication and there has been no significant financial support for this work that could have influenced its outcome.

Data availability

The data that has been used is confidential.

Acknowledgements

The work carried out by FG has been supported by projects CGL2017-85045-P and DIAPERNO PID2021-123189NB-I00 (Spanish Government). EG has been supported by The Scientific and Technological Research Council of Turkey (TÜBİTAK) under the International Research Fellowship Programme for Ph.D. students (BİDEB 2214-A). We thank the editor Martin Stokes and the reviewers Laurent Bruxelles, Ognjen Bonacci and Tony Waltham for their constructive comments.

References

Aiello, G., Ascione, A., Barra, D., Munno, R., Petrosino, P., Ermolli, E.R., Villani, F., 2007. Evolution of the late Quaternary San Gregorio Magno tectono-karstic basin (southern Italy) inferred from geomorphological, tephrostratigraphical and palaeoecological analyses: tectonic implications. J. Quat. Sci. 22 (3), 233–245. https://doi.org/10.1002/jqs.1040.

Alagöz, C.A., 1967. In: Sivas çevresi ve doğusunda jips karstı olayları, 175. Ankara Üniversitesi Dil ve Tarih-Coğrafya Fakültesi Yayını, p. 126.

Andrejchuk, V., Klimchouk, A., 2002. Mechanisms of karst breakdown formation in the gypsum karst of the fore-Ural region, Russia (from observations in the Kungurskaja Cave). Int. J. Speleol. 31, 89–114. https://doi.org/10.5038/1827-806X.31.1.5.

Bayrakdar, C., Döker, M.F., Keserci, F., 2020. Polyelerde Hatalı Arazi Kullanımların Sebep Olduğu Afetlere Bir Örnek: 31 Ocak 2019 Kayaköy Polyesi Taşkını. Coğrafya Dergisi 41. https://doi.org/10.26650/JGEOG2020-0046.

Blatnik, M., Frantar, P., Kosec, D., Gabrovšek, F., 2017. Measurements of the outflow along the eastern border of Planinsko Polje, Slovenia. Acta Carsologica 46 (1), 83–93. https://doi.org/10.3986/ac.v46i1.4774.

Bonacci, O., 1987. Karst Hydrology with Special References to the Dinaric Karst. Springer, Berlin. https://doi.org/10.1007/978-3-642-83165-2.

Bonacci, O., 2004. Poljes. In: Gunn, J. (Ed.), Encyclopedia of Caves and Karst Science. Fitzroy Dearborn, New York, pp. 599–600.

Bonacci, O., 2013. Poljes, ponors and their catchments. In: Shroder, J.F. (Ed.), Treatise on Geomorphology. Academic Press, San Diego, pp. 112–120. https://doi.org/10.1016/B978-0-12-374739-6.00103-2.

Bruxelles, L., Simon-Coiçon, R., Guendon, J.-L., Ambert, P., 2007. Formes et formations superficielles de la partie Ouest du Causse de Sauveterre (Grands Causses). Karstologia 49, 1–14. https://doi.org/10.3406/karst.2007.2595.

Calaforra, J.M., Pulido-Bosch, A., 1999. Gypsum karst features as evidence of diapiric processes in the Betic Cordillera, Southern Spain. Geomorphology 29 (3), 251–264. https://doi.org/10.1016/S0169-555X(99)00019-7.

Cvijić, J., 1893. In: Das Karstphänomen. Versuch einer morphologischen Monographie. Geographische Abhandlungen herausgegeben von A. Penck, Wien, p. 114. PhD Thesis.

Cvijić, J., 1918. Hydrographie souterraine et évolution morphologique du Karst. In: Recueil des travaux de l'institut de géographie alpine, 6, pp. 375–426.

Darin, M.H., Umhoefer, P.J., Thomson, S.N., 2018. Rapid Late Eocene exhumation of the Sivas Basin (Central Anatolia) driven by initial Arabia-Eurasia Collision. Tectonics 37 (10), 3805–3833. https://doi.org/10.1029/2017TC004954.

De Waele, J., Gutiérrez, F., 2022. Karst Hydrogeology, Geomorphology and Caves. Wiley-Blackwell, Chichester.

De Waele, J., Piccini, L., Columbu, A., Madonia, G., Vattano, M., Calligaris, C., D'Angeli, I.M., Parise, M., Chiesi, M., Sivelli, M., Vigna, B., Zini, L., Chiarini, V., Sauro, F., Drysdale, R., Forti, P., 2017. Evaporite karst in Italy: a review. Int. J. Speleol. 46 (2), 137–168. https://doi.org/10.5038/1827-806X.46.2.2107.

Doğan, U., Özel, S., 2005. Gypsum karst and its evolution east of Hafik (Sivas, Turkey). Geomorphology 71 (3), 373–388. https://doi.org/10.1016/j.geomorph.2005.04.009.

Doğan, U., Yeşilyurt, S., 2004. Gypsum karst south of İmranlı. Cave Karst Sci. 31 (1), 7–14.

Doğan, U., Yeşilyurt, S., 2019. Gypsum karst landscape in the Sivas Basin. In: Kuzucuoğlu, C., Çiner, A., Kazancı, N. (Eds.), Landscapes and Landforms of Turkey. World Geomorphological Landscapes. Springer International Publishing, Cham, pp. 197–206. https://doi.org/10.1007/978-3-030-03515-0_6.

Doğan, U., Koçyiğit, A., Gökkaya, E., 2017. Development of the Kembos and Eynif structural poljes: morphotectonic evolution of the Upper Manavgat River basin, central Taurides, Turkey. Geomorphology 278, 105–120. https://doi.org/10.1016/j.geomorph.2016.10.030.

Doğan, U., Koçyiğit, A., Yeşilyurt, S., 2019. The relationship between Kestel Polje system and the Antalya Tufa Plateau: their morphotectonic evolution in Isparta Angle, Antalya-Turkey. Geomorphology 334, 112–125. https://doi.org/10.1016/j.geomorph.2019.03.003.

Fabre, G., Nicod, J., 1982. Modalités et rôle de la corrosion crypto-karstique dans les karsts méditerranéens et tropicaux. Z. Geomorphol. 26, 209–224.

Field, M., 2002. A Lexicon of Cave and Karst Terminology With Special Reference to Environmental Karst Hydrology. EPA National Center for Environmental Assessment, Washington, D.C.

Ford, D., Williams, P., 2007. Karst Hydrogeology and Geomorphology. John Wiley & Sons, Chichester.

Franz, N., Sorokin, S., Alexeeva, A., Inshina, I., Novysh, O., Kazak, A., 2013. field measurements of gypsum denudation rate in Kulogorskaya Cave System. In: Filippi, M., Bosák, P. (Eds.), Proceedings of the 16th International Congress of Speleology, Czech Republic, Brno, pp. 185–193.

Frumkin, A., 2013. Salt karst. In: Shroder, J.F. (Ed.), Treatise on Geomorphology. Academic Press, San Diego, pp. 407–424. https://doi.org/10.1016/B978-0-12-374739-6.00113-5.

Gams, I., 1978. The Polje: the problem of definition. Z. Geomorphol. 22, 170–181.

Gams, I., 1994. Types of the poljes in Slovenia, their inundations and land use. Acta Carsologica 23, 285–302.

Garay, P., 2001. In: El dominio triásico Espadán-Calderona. Contribución a su conocimiento geológico e hirogeológico. University of Valencia, p. 692. PhD Thesis Thesis.

Gökkaya, E., Gutiérrez, F., Ferk, M., Görüm, T., 2021. Sinkhole development in the Sivas gypsum karst, Turkey. Geomorphology 386, 107746. https://doi.org/10.1016/j.geomorph.2021.107746.

Gracia, F.J., Gutiérrez, F., Gutiérrez, M., 2002. Origin and evolution of the Gallocanta Polje. Z. Geomorphol. 46 (2), 245–262.

Gracia, F.J., Gutiérrez, F., Gutiérrez, M., 2003. The Jiloca karst Polje-tectonic graben (Iberian Range, NE Spain). Geomorphology 52 (3), 215–231. https://doi.org/10.1127/zfg/46/2002/245.

Guerrero, J., Gutiérrez, F., Lucha, P., 2008. Impact of halite dissolution subsidence on Quaternary fluvial terrace development: Case study of the Huerva River, Ebro Basin, NE Spain. Geomorphology 100 (1), 164–179. https://doi.org/10.1016/j.geomorph.2007.04.040.

Günay, G., 2002. Gypsum karst, Sivas, Turkey. Environ. Geol. 42 (4), 387–398. https://doi.org/10.1007/s00254-002-0532-0.

Gündoğan, I., Önal, M., Depçi, T., 2005. Sedimentology, petrography and diagenesis of Eocene–Oligocene evaporites: the Tuzhisar Formation, SW Sivas Basin, Turkey. Journal of Asian Earth Sciences 25 (5), 791–803. https://doi.org/10.1016/j.jseaes.2004.08.002.

Gürsoy, H., Temiz, H., Poisson, A., 1992. Recent faulting in the Sivas area (Sivas Basin, Central Anatolia—Turkey). Bull. Faculty Eng. Cumhuriyet Univ., A 9, 11–17.

Gutiérrez, F., 1998. PhD Thesis Thesis. In: Fenómenos de subsidencia por disolución de formaciones evaporíticas en las fosas neógenas de Calatayud y Teruel (Cordillera Ibérica). University of Zaragoza, p. 569.

Gutiérrez, F., 2014. Evaporite karst in Calatayud, Iberian Chain. In: Gutiérrez, F., Gutiérrez, M. (Eds.), Landscapes and Landforms of Spain. World Geomorphological Landscapes. Springer, Netherlands, Dordrecht, pp. 111–125. https://doi.org/10.1007/978-94-017-8628-7_9.

Gutiérrez, F., 2016. Sinkhole hazards. In: Cutter, S.L. (Ed.), Oxford Research Encyclopedia of Natural Hazard Science. Oxford University Press, pp. 1–92. https://doi.org/10.1093/acrefore/9780199389407.013.40.

Gutiérrez, F., Cooper, A.H., 2013. Surface morphology of gypsum karst. In: Shroder, J.F. (Ed.), Treatise on Geomorphology. Academic Press, San Diego, pp. 425–437. https://doi.org/10.1016/B978-0-12-374739-6.00114-7.

Gutiérrez, F., Calaforra, J.M., Cardona, F., Ortí, F., Durán, J.J., Garay, P., 2008a. Geological and environmental implications of the evaporite karst in Spain. Environ. Geol. 53 (5), 951–965. https://doi.org/10.1007/s00254-007-0721-y.

Gutiérrez, F., Guerrero, J., Lucha, P., 2008b. A genetic classification of sinkholes illustrated from evaporite paleokarst exposures in Spain. Environ. Geol. 53 (5), 993–1006. https://doi.org/10.1007/s00254-007-0727-5.

Jackson, M.P., Hudec, M.R., 2017. Salt Tectonics: Principles and Practice. Cambridge University Press.

James, A.N., Cooper, A.H., Holliday, D.W., 1981. Solution of the gypsum cliff (Permian, Middle Marl) by the River Ure at Ripon Parks, North Yorkshire. Proc. Yorks. Geol. Soc. 43 (4), 433–450. https://doi.org/10.1144/pygs.43.4.433.

Johnson, S.Y., 1986. Water-escape structures in coarse-grained, volcaniclastic, fluvial deposits of the Ellensburg Formation, south-central Washington. J. Sediment. Petrol. 56 (6), 905–910. https://doi.org/10.1306/212F8A80-2B24-11D7-8648000102C1865D.

Kaçaroğlu, F., Değirmenci, M., Cerit, O., 2001. Water quality problems of a gypsiferous watershed: Upper Kizilirmak Basin, Sivas, Turkey. Water Air Soil Pollut. 128, 161–180. https://doi.org/10.1023/A:1010333522184.

Kergaravat, C., Ribes, C., Legeay, E., Callot, J.-P., Kavak, K.S., Ringenbach, J.-C., 2016. Minibasins and salt canopy in foreland fold-and-thrust belts: the central Sivas Basin, Turkey. Tectonics 35 (6), 1342–1366. https://doi.org/10.1002/2016TC004186.

Kergaravat, C., Ribes, C., Callot, J.-P., Ringenbach, J.-C., 2017. Tectono-stratigraphic evolution of salt-controlled minibasins in a fold and thrust belt, the Oligo-Miocene Central Sivas Basin. J. Struct. Geol. 102, 75–97. https://doi.org/10.1016/j.jsg.2017.07.007.

Klimchouk, A.B., Aksem, S.D., 2005. Hydrochemistry and solution rates in gypsum karst: case study from the Western Ukraine. Environ. Geol. 48 (3), 307–319. https://doi.org/10.1007/s00254-005-1277-3.

Klimchouk, A., Cucchi, F., Calaforra, J.M., Aksem, S., Finocchiaro, F., Forti, P., 1996. Dissolution of gypsum from field observations. Int. J. Speleol. 25 (3), 37–48. https://doi.org/10.5038/1827-806X.25.3.3.

Legeay, E., Pichat, A., Kergaravat, C., Ribes, C., Callot, J.P., Ringenbach, J.C., Bonnel, C., Hoareau, G., Poisson, A., Mohn, G., Crumeyrolle, P., Kavak, K.S., Temiz, H., 2019a. Geology of the Central Sivas Basin (Turkey). J. Maps 15 (2), 406–417. https://doi.org/10.1080/17445647.2018.1514539.

Legeay, E., Ringenbach, J.-C., Kergaravat, C., Pichat, A., Mohn, G., Vergés, J., Kavak, K. S., Callot, J.-P., 2019b. Structure and kinematics of the Central Sivas Basin (Turkey):

salt deposition and tectonics in an evolving fold-and-thrust belt. Geol. Soc. Lond., Spec. Publ. 490, 361–396. https://doi.org/10.1144/SP490-2019-92.
López-Chicano, M., Calvache, M.L., Martín-Rosales, W., Gisbert, J., 2002. Conditioning factors in flooding of karstic poljes—the case of the Zafarraya polje (South Spain). Catena 49 (4), 331–352. https://doi.org/10.1016/S0341-8162(02)00053-X.
Lundberg, J., 2019. Karren, cave. In: White, W.B., Culver, D.C., Pipan, T. (Eds.), Encyclopedia of Caves, Third edition. Academic Press, pp. 588–599. https://doi.org/10.1016/B978-0-12-814124-3.00070-4.
Mayer, D.V., 1973. In: All List Some of the Caves and Swallow Holes in the Gypsum Karst Between Sivas and Zara, Turkey, Unpublished Notes. BCRA Library, p. 7.
Mayer, D.V., 1974. Gypsum caves in Turkey. BCRABulletin 3, 15–16.
McQuarrie, N., Hinsbergen, D.J.J., 2013. Retrodeforming the Arabia-Eurasia collision zone: age of collision versus magnitude of continental subduction. Geology 41 (3), 315–318. https://doi.org/10.1130/g33591.1.
Mijatović, B.F., 1984. Karst poljes in the Dinarides. In: Mijatović, B.F. (Ed.), Hydrogeology of the Dinaric Karst. International Association of Hydrogeologists, Hannover, pp. 87–109.
Milanovic, P., 2002. The environmental impacts of human activities and engineering constructions in karst regions. Int. Union Geol. Sci. 25 (1), 13–21. https://doi.org/10.18814/epiiugs/2002/v25i1/002.
Milanovic, P., 2018. In: Engineering Karstology of Dams and Reservoirs. CRC Press, Boca Raton, p. 368. https://doi.org/10.1201/9780429453403.
Nicod, J., 1975. Corrosion de type crypto-karstique dans les karsts méditerranéens. Bulletin de l'Association de Géographes Français 428, 289–297.
Nicod, J., 2006. Lakes in gypsum karst: some examples in Alpine and Mediterranean countries. Acta Carsologica 35 (1), 69–78. https://doi.org/10.3986/ac.v35i1.244.
Nocita, B.W., 1988. Soft-sediment deformation (fluid escape) features in a coarse-grained pyroclastic-surge deposit, north-central New Mexico. Sedimentology 35 (2), 275–285. https://doi.org/10.1111/j.1365-3091.1988.tb00949.x.
Önal, M., Demir, O., Öztaş, Y., 1999. Uzunyayla baseninin jeolojisi ve hidrokarbon olanakları, Unpublished Report No. 3984, 76.
Palmer, A.N., 1991. Origin and morphology of limestone caves. Geol. Soc. Am. Bull. 103 (1), 1–21. https://doi.org/10.1130/0016-7606(1991)103<0001:Oamolc>2.3.Co;2.
Palmer, A.N., 2007. In: Cave Geology. Cave Books, Dayton, Ohio, p. 454.
Panno, S.V., Luman, D.E., 2018. Characterization of cover-collapse sinkhole morphology on a groundwater basin-wide scale using lidar elevation data: a new conceptual model for sinkhole evolution. Geomorphology 318, 1–17. https://doi.org/10.1016/j.geomorph.2018.05.013.
Pechorkin, I.A., 1969. Geodynamic of Coasts of the Kama Reservoirs (in Russian).
Phillips, J.D., 2017. Landform transitions in a fluviokarst landscape. Z. Geomorphol. 61 (2), 109–122. https://doi.org/10.1127/zfg/2017/0452.
Pichat, A., 2017. Dynamique des systèmes évaporitiques d'un bassin d'avant-pays salifère et processus diagénétiques associés au contexte halocinétique: exemple du bassin de Sivas en Turquie. Université de Pau et des Pays de l'Adour, France.
Pichat, A., Hoareau, G., Callot, J.-P., Legeay, E., Kavak, K.S., Révillon, S., Parat, C., Ringenbach, J.-C., 2018. Evidence of multiple evaporite recycling processes in a salt-tectonic context, Sivas Basin, Turkey. Terra Nova 30 (1), 40–49. https://doi.org/10.1111/ter.12306.
Poisson, A., Guezou, J.C., Ozturk, A., Inan, S., Temiz, H., Gürsöy, H., Kavak, K.S., Özden, S., 1996. Tectonic setting and evolution of the Sivas Basin, Central Anatolia, Turkey. International Geology Review 38 (9), 838–853. https://doi.org/10.1080/00206819709465366.
Poisson, A., Orszag-sperber, F., Temiz, H., Vrielynck, B., 2011. In: Stratigraphic and Polyphased Tectonic Evolution of the Sivas Basin (Central Anatolia, Turkey), Darius Annual Report 2011 - Proposal No WD 11-11, pp. 1–29.
Poisson, A., Vrielynck, B., Wernli, R., Negri, A., Bassetti, M.-A., Büyükmeriç, Y., Özer, S., Guillou, H., Kavak, K.S., Temiz, H., Orszag-Sperber, F., 2016. Miocene transgression in the central and eastern parts of the Sivas Basin (Central Anatolia, Turkey) and the Cenozoic palaeogeographical evolution. Int. J. Earth Sci. 105 (1), 339–368. https://doi.org/10.1007/s00531-015-1248-1.
Postma, G., 1983. Water escape structures in the context of a depositional model of a mass flow dominated conglomeratic fan-delta (Abrioja Formation, Pliocene, Almeria Basin, SE Spain). Sedimentology 30 (1), 91–103. https://doi.org/10.1111/j.1365-3091.1983.tb00652.x.
Poyraz, M., Öztürk, M.Z., Soykan, A., 2021. Sivas jips karstında dolin yoğunluğunun CBS tabanlı analizi. Jeomorfolojik Araştırmalar Dergisi 6, 67–80. https://doi.org/10.46453/jader.863090.
Ribes, C., Kergaravat, C., Bonnel, C., Crumeyrolle, P., Callot, J.-P., Poisson, A., Temiz, H., Ringenbach, J.-C., 2015. Fluvial sedimentation in a salt-controlled mini-basin: stratal patterns and facies assemblages, Sivas Basin, Turkey. Sedimentology 62 (6), 1513–1545. https://doi.org/10.1111/sed.12195.
Ribes, C., Kergaravat, C., Crumeyrolle, P., Lopez, M., Bonnel, C., Poisson, A., Kavak, K.S., Callot, J.-P., Ringenbach, J.-C., 2017. Factors controlling stratal pattern and facies distribution of fluvio-lacustrine sedimentation in the Sivas mini-basins, Oligocene (Turkey). Basin Res. 29 (S1), 596–621. https://doi.org/10.1111/bre.12171.
Sanz de Galdeano, C., 2013. The Zafarraya Polje (Betic Cordillera, Granada, Spain), a basin open by lateral displacement and bending. J. Geodyn. 64, 62–70. https://doi.org/10.1016/j.jog.2012.10.004.
Sauro, U., 1996. Geomorphological aspects of gypsum karst areas with special emphasis on exposed karst. Int. J. Speleol. 25, 105–114. https://doi.org/10.5038/1827-806X.25.3.8.
Sivinskih, P., 2009. Features of geological conditions of the Ordinskaya underwater cave, fore-Urals, Russia. In: Klimchouk, A., Derek, F. (Eds.), Hypogene Speleogenesis and Karst Hydrogeology of Artesian Basins. Ukrainian Institute of Speleology and Karstology, Simferopol, pp. 267–269.
Stepišnik, U., Ferk, M., Gostinčar, P., Černuta, L., 2012. Holocene high floods on the Planina Polje, Classical Dinaric Karst, Slovenia. Acta Carsologica 41 (1). https://doi.org/10.3986/ac.v41i1.44.
Sümengen, M., Ünay, E., Sarac, G., de Bruijn, H., Terlemez, I., Gürbüz, M., 1990. New neogene rodent assemblages from Anatolia (Turkey). In: Lindsay, E.H., Fahlbusch, V., Mein, P. (Eds.), European Neogene Mammal Chronology. NATO Advanced Science Institutes Series. Plenum Press, New York, pp. 515–525. https://doi.org/10.1007/978-1-4899-2513-8_5.
Sweeting, M.M., 1972. Karst Landforms. McMillan Press, London.
Temiz, H., 1996. Tectonostratigraphy and thrust tectonics of the Central and Eastern parts of the Sivas Tertiary Basin, Turkey. International Geology Review 38 (10), 957–971. https://doi.org/10.1080/00206819709465374.
Waltham, T., 2002. Gypsum karst near Sivas, Turkey. Cave Karst Sci. 29 (1), 39–44.
Warren, J.K., 2016. Evaporites: A Geological Compendium. Springer. https://doi.org/10.1007/978-3-319-13512-0.